ELSEVIER

Progress in Biophysics & Molecular Biology 88 (2005) 59–90

Progress in Biophysics & Molecular Biology

www.elsevier.com/locate/pbiomolbio

Review

# Axonal excitability revisited

John R. Clay*

*Ion Channel Biophysics Group, National Institute of Neurological Disorders and Stroke, National Institutes of Health, Building 36 Room 4A21, 9000 Rockville Pike, Bethesda, MD 20892, USA*

**Abstract**

The original papers of Hodgkin and Huxley (J. Physiol. 116 (1952a) 449, J. Physiol. 116 (1952b) 473, J. Physiol. 116 (1952c) 497, J. Physiol. 117 (1952d) 500) have provided a benchmark in our understanding of cellular excitability. Not surprisingly, their model of the membrane action potential (AP) requires revisions even for the squid giant axon, the preparation for which it was originally formulated. The mechanisms they proposed for the voltage-gated potassium and sodium ion currents, $I_K$, and $I_{Na}$, respectively, have been superceded by more recent formulations that more accurately describe voltage-clamp measurements of these components. Moreover, the current–voltage relation for $I_K$ has a non-linear dependence upon driving force that is well described by the Goldman–Hodgkin–Katz (GHK) relation, rather than the linear dependence on driving force found by Hodgkin and Huxley. Furthermore, accumulation of potassium ions in the extracellular space adjacent to the axolemma appears to be significant even during a single AP. This paper describes the influence of these various modifications in their model on the mathematically reconstructed AP. The GHK and $K^+$ accumulation results alter the shape of the AP, whereas the modifications in $I_K$ and $I_{Na}$ gating have surprisingly little effect. Perhaps the most significant change in their model concerns the amplitude of $I_{Na}$, which they appear to have overestimated by a factor of two. This modification together with the GHK and the $K^+$ accumulation results largely remove the discrepancies between membrane excitability of the squid giant axon and the Hodgkin and Huxley (J. Physiol. 117 (1952d) 500) model previously described (Clay, J. Neurophysiol. 80 (1998) 903).
Published by Elsevier Ltd.

*Keywords:* Action potential; $K^+$ and $Na^+$ channels; Mathematical models

**Contents**



*Fax: +1-301-402-1565.
*E-mail address:* jrclay@ninds.nih.gov (J.R. Clay).

0079-6107/$ - see front matter Published by Elsevier Ltd.
doi:10.1016/j.pbiomolbio.2003.12.004

## 1. Introduction

Over 50 years ago, Hodgkin and Huxley (1952a–d) published a series of papers that have provided a fundamental, conceptual framework in neuroscience concerning membrane excitability, i.e., the mechanisms responsible for initiation and propagation of the nerve impulse along axonal processes. Their work can be divided into two parts—analysis and synthesis. The analysis portion concerns the use of the voltage-clamp technique to determine the ionic current mechanisms that underlie the nerve impulse, specifically the potassium ion current, $I_K$, the sodium ion current, $I_{Na}$, and the leak component, $I_L$. The synthesis portion concerns mathematical descriptions of the currents, and finally, a reconstruction of the impulse—the action potential (AP)—from those descriptions using numerical techniques. This work has been so successful that their equations continue to be used by computational neuroscientists even though several studies have demonstrated that revisions are required in their model. Moreover, the emphasis on the voltage-clamp methodology in the decades following publication of the Hodgkin and Huxley (1952a–d) papers overshadowed their theoretical analysis. In particular, relatively little work has been carried out concerning the effects of revised descriptions of $I_K$ and $I_{Na}$ on axonal excitability.

The purpose of this review is to recapitulate those revisions and to assess their effects on the mathematically reconstructed AP. The focus is on the squid giant axon since this preparation has provided the most detailed set of experimental results for any preparation concerning $I_K$ and $I_{Na}$ at both the macroscopic, or whole-cell level, and at the level of single channel and gating current measurements. Moreover, most axons contain the currents found in the squid giant axon—$I_K$, $I_{Na}$, and $I_L$. Consequently, conclusions drawn from those results may, with a few exceptions, be relevant for all axons.

## 2. Revisions in the HH model

### 2.1. Potassium ion current, $I_K$—ion permeation

#### 2.1.1. Current–voltage relation (IV curve)

One of the assumptions of the HH model, based on their voltage-clamp measurements, is that ionic currents are described by $I = g(V–E)$, where $V$ is the membrane potential, $E$ is the reversal potential for the ionic component in question, and $g$ is its conductance, which for $I_K$ and $I_{Na}$, is both time- and voltage-dependent. Other work, beginning with that of Frankenhauser (1962) on frog myelinated axons, has shown that $I_K$ has a non-linear dependence on the driving force ($V–E_K$), a non-linearity that is well described by the Goldman–Hodgkin–Katz (GHK) equation (Goldman, 1943; Hodgkin and Katz, 1949). A similar result was reported for $I_K$ in *Myxicola* giant axons (Binstock and Goldman, 1971) and for other $K^+$ channels, including the squid giant axon $I_K$ (Clay, 1991, 2000). The $K^+$ channel $IV$ relationship outwardly rectifies (Fig. 1). That is, it curves upward with increasing membrane depolarization, consistent with the observation that the $K^+$ concentration inside the axon is significantly larger than it is outside.

Consequently, a requisite change in the HH model is that $I_K$ should be given by

$$I_K = g_K V(\exp(q(V - E_K) - 1)/(\exp(qV/kT - 1), \tag{1}$$

instead of $I_K = g_K(V–E_K)$, where $q$ is the unit electronic charge, $k$ is the Boltzmann constant, and $T$ is the absolute temperature. (The constants $q$ and $k$ are used here rather than $F$ and $R$, where $F$ and $R$ are the Faraday and the gas constants, respectively. Note that $q/k = F/R$.) The quantity $kT/q = 24\,\text{mV}$ for $T = 6°\text{C}$, the temperature used in the experiments reviewed in this report.

#### 2.1.2. The IV curve and $g_K$ are inter-related

The change in the current–voltage relation for $I_K$ noted above requires a concomitant change in $g_K$. Hodgkin and Huxley (1952a, b) determined the activation curve for $I_K$, sometimes referred to as the $g_K–V$ curve, by factoring out the driving force from their $I_K$ results (Fig. 2, taken from Clay, 1998). Voltage-clamp records of $I_K$ from squid giant axons are illustrated in the left upper panel of Fig. 2. The currents at the end of these steps, $I_o$, when normalized by ($V–E_K$), give a weakly voltage-dependent relationship (dashed curve in the middle panel of Fig. 2). This result corresponds to $n_\infty^4(V)$ in the HH model with $n_\infty(V) = \alpha_n/(\alpha_n + \beta_n)$, where $\alpha_n = -0.01(V + 50)/(\exp(-0.1(V + 50)) - 1)\,\text{ms}^{-1}$ and $\beta_n = 0.125\exp(-(V + 60)/80)\,\text{ms}^{-1}$. Normalization of the $I_o$ results by the GHK dependence on ($V–E_K$) yields the data points shown in the middle panel of Fig. 2. These results are well described by $n_\infty^4(V)$ with $\alpha_n$ the same as in the HH

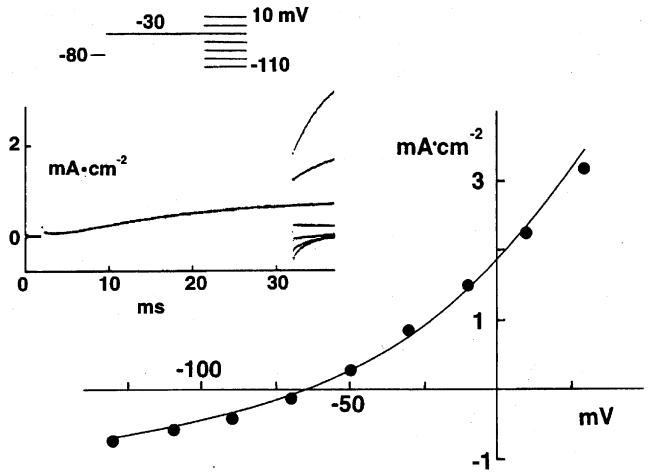


Fig. 1. $K^+$ channel current–voltage relation from squid axons. Inset: The membrane potential was stepped to −30 mV for 30 ms from a holding potential of −80 mV to activate the $K^+$ conductance. This modest level of depolarization was chosen so as to minimize accumulation of K ions in the extracellular space. The potential was then stepped to the levels indicated. A 3 s rest interval was used between each two step sequence in the protocol. TTX was used to block $I_{Na}$. The currents immediately following the second step are plotted here. The curve represents the best fit to these results of the GHK equation, $aV(\exp(V - E_K)/24) - 1)/(\exp(V/24) - 1)$, where $a$ is a constant and $E_K = -65$ mV. The predicted $E_K$ is −82 mV. This difference is attributable to small degree of accumulation of $K^+$ in the extracellular space, which is unavoidable in these experiments even with modest depolarizations. Further details are given in Clay and Shlesinger (1983).

model, but with $\beta_n$ changed to $0.1\exp(-(V + 60)/25)\,\mathrm{ms}^{-1}$. (The major change here is the "25" in the denominator of the exponent, as compared to "80" in the HH model.) This relationship has a significantly steeper voltage dependence than the original $n^4_\infty(V)$ curve. As noted recently by Sigworth (2003), ion channels are very sensitive to changes of membrane potential in the physiological range, moreso than physical devices such as transistors. The original $n^4_\infty(V)$ curve in the HH model has a voltage dependence similar to that of a transistor. However, relatively minor changes in their $\beta_n$ term can adequately describe the revised $g_K$–$V$ results (Fig. 2, middle panel). The $g_K$–$V$ curves of other voltage-gated $K^+$ channels have a steepness similar to that of the revised squid results (Clay, 2000).

### 2.1.3. *Modifications in $I_K$—consequences for the action potential*

An assessment of the effects of the changes in $I_K$ on the AP requires a brief recapitulation of the HH model. The model is given by

$$dV/dt = -C^{-1}(I_K + I_{Na} + I_L + I_{stim}), \tag{2}$$

where $C$ is the membrane capacitance ($1\,\mu F/cm^2$); $I_K$, $I_{Na}$, and $I_L$ are the $K^+$, $Na^+$, and leak currents, respectively; and $I_{stim}$ is the stimulus current. (All currents are in units of $\mu A/cm^2$, $V$ is in mV, and $t$ is in ms.) The $I_K$ component is given by

$$I_K = g'_K n^4(V, t)(V - E_K), \tag{3}$$

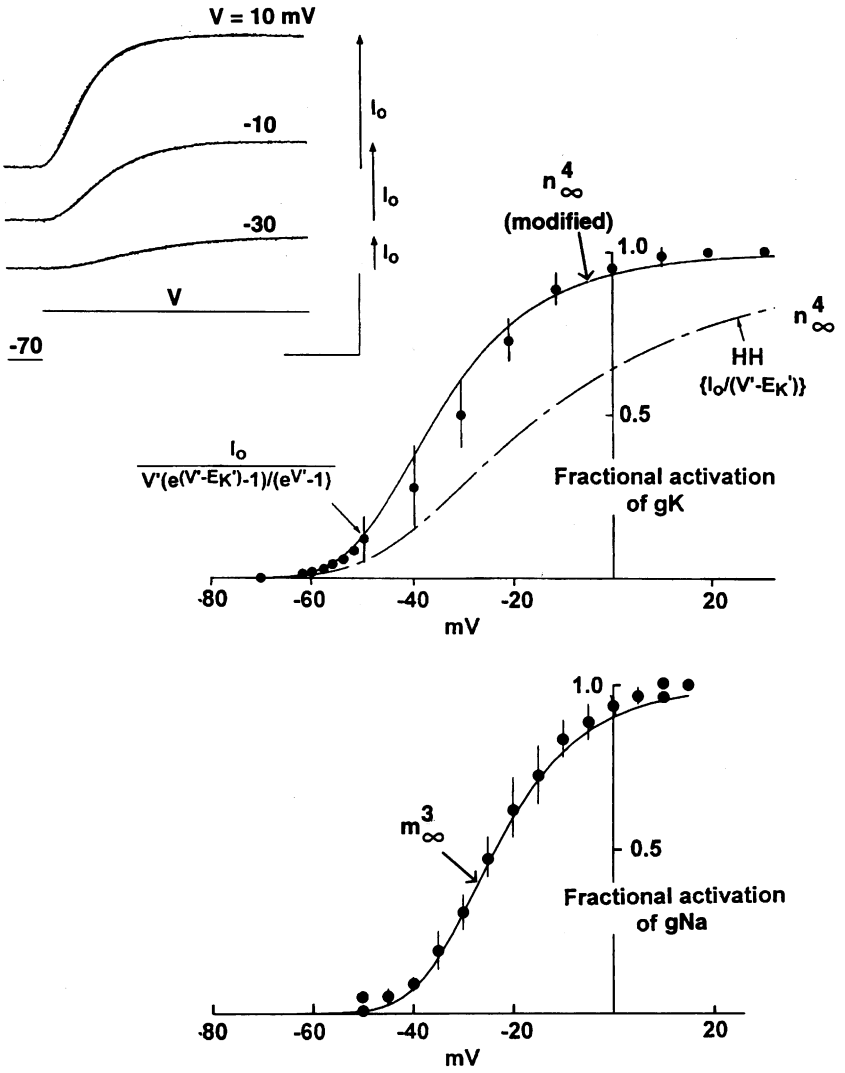


Fig. 2. Steady-state activation of $I_K$. The records in the upper inset were obtained with TTX in the external solution. The calibrations represent 5 ms and 1 mA/cm$^2$, respectively. The currents at the end of these steps, $I_o$, were normalized by the GHK equation to given the experimental points in the middle panel. The line through these results represents $n^4_\infty(V)$ with $\alpha_n$ as given by HH and $\beta_n = 0.1\exp(-(V+60)/25)\,\mathrm{ms}^{-1}$. The dashed curve represents $n^4_\infty(V)$ as given by HH with their $\beta_n$, which is given by $0.125\exp(-(V+60)/80)\,\mathrm{ms}^{-1}$. Bottom panel: Measurements of $I_{Na}$ activation in squid giant axons with inactivation removed by *N*-bromoacetamide (Oxford, 1981). The solid line represents $m^3_\infty$ from HH, where $m_\infty = \alpha_m/(\alpha_m+\beta_m)$, with $\alpha_m = -0.1(V+35)/(\exp(-0.1(V+35))-1)\,\mathrm{ms}^{-1}$ and $\beta_m = 4\exp(-(V+60)/18)\,\mathrm{ms}^{-1}$.

where $g'_K = 36\,\mathrm{mS/cm}^2$, $E_K = -72\,\mathrm{mV}$ (arbitrarily chosen by HH to be 12 mV below the rest potential), and $\mathrm{d}n(V,t) = -(\alpha_n+\beta_n)n(V,t)+\alpha_n$, with $\alpha_n = -0.01(V+50)/(\exp(-0.1(V+50))-1)\,\mathrm{ms}^{-1}$ and $\beta_n = 0.125\exp(-(V+60)/80)\,\mathrm{ms}^{-1}$.

The revised $I_K$ is given by

$$I_K = g'_K Vn^4(V,t)(\exp((V - E_K)/24) - 1)/(\exp(V/24) - 1), \quad (4)$$

where $g'_K = 2\,\mathrm{mS/cm^2}$, $E_K = -82\,\mathrm{mV}$ (using $K_o = 10\,\mathrm{mM}$ and $K_i = 300\,\mathrm{mM}$), $\alpha_n$ as given by HH, and $\beta_n = 0.1\exp(-(V + 60)/25)\,\mathrm{ms^{-1}}$. Eqs. (3) and (4) both predict a current amplitude of approximately $1.5\,\mathrm{mA/cm^2}$ at the end of a 20 ms voltage-clamp step to 0 mV from a holding potential of −60 mV, which is consistent with experimental recordings. The $I_{Na}$ component is given by

$$I_{Na} = g'_{Na} m^3(V,t)h(V,t)(V - E_{Na}), \quad (5)$$

where $g'_{Na} = 120\,\mathrm{mS/cm^2}$, $E_{Na} = 55\,\mathrm{mV}$, $\mathrm{d}m(V,t) = -(\alpha_m + \beta_m)m(V,t) + \alpha_m$, and $\mathrm{d}h(V,t) = -(\alpha_h + \beta_h)h(V,t) + \alpha_h$, where $\alpha_m = -0.1(V + 35)/(\exp(-0.1(V + 35)) - 1)\,\mathrm{ms^{-1}}$, $\beta_m = 4\exp(-(V + 60)/18)\,\mathrm{ms^{-1}}$, $\alpha_h = 0.07\exp(-(V + 60)/20)\,\mathrm{ms^{-1}}$, and $\beta_h = 1/(\exp(-0.1(V + 30)) + 1)\,\mathrm{ms^{-1}}$. The leak component, $I_L$, is given by $0.3(V + 49)$. The responses of the original HH model (hereafter referred to simply as HH) and the HH model with the revised description of $I_K$ are illustrated in Fig. 3B and C, respectively, for a 1 ms duration suprathreshold current pulse, along with a representative recording of an AP (Fig. 3A). (Details of these results are provided in the legend of Fig. 3.) The rising phase and the initial portion of the repolarization phase of both models compare favorably with the experimental result. However, the membrane potential in HH sharply changes direction at the foot of the voltage waveform, as indicated by the arrow in Fig. 3B, which is unlike the experimental recording. This result is directly attributable to the linear dependence of $I_K$ on $(V - E_K)$. A relatively large fraction of $K^+$ channels are open during the repolarization phase and so the membrane potential is rapidly driven toward $E_K$ because of the

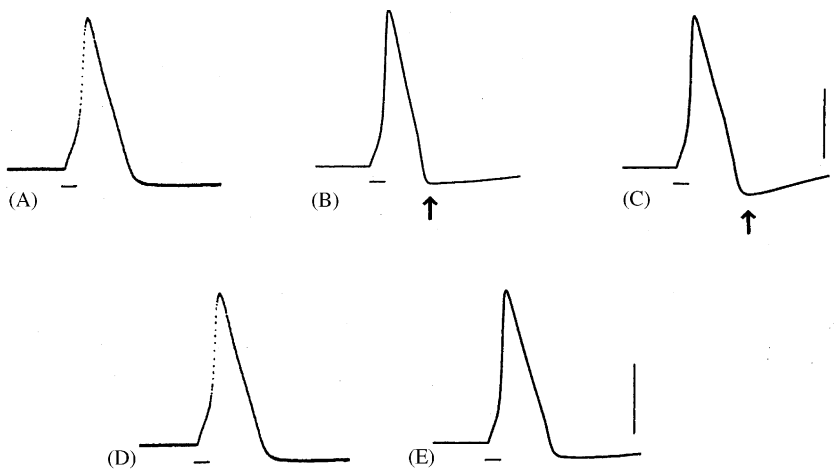


Fig. 3. Action potential responses to brief duration current pulses. (A, D) Experimental recording from a squid giant axon in response to a $30\,\mu\mathrm{A/cm^2}$ current pulse 1 ms in duration (indicated by the bar below the record). $T = 6^\circ\mathrm{C}$. Same record in (A) and (D). (B, C, E) Action potentials simulated from the HH model, the HH model with the revised $I_K$ without the accumulation/depletion effect, and the HH model with the revised $I_K$ including accumulation/depletion, respectively. Same stimulus conditions as in (A) and (D). The calibration in (C) and (E) represents 50 mV. The top of the bar corresponds to 0 mV. The simulations were carried out with the Mathematica software package (Wolfram, 1999).

linear dependence of $I_K$ on driving force, moreso than in the experimental recording or in the model with the GHK dependence on driving force. Moreover, the model with the revised version of $I_K$ repolarizes to −80 mV (Fig. 3C), as compared to −70 mV (Fig. 3A), where it remained for several ms. Throughout this time the dominant membrane current is $I_K$, which suggests that the membrane potential is effectively at $E_K$. This 10 mV difference from the theoretical $E_K$ can be accounted for by accumulation of K ions in the space external to the axolemma, as described in the following section.

### 2.1.4. *Accumulation–depletion of $K^+$ in the extracellular space*

The giant axon is surrounded by several barriers, the basement membrane and a glial cell layer in particular (Adelman et al., 1977), which can impede the movement of K ions from inside the cell to the external bathing medium during electrical activity and voltage-clamp depolarizations. Consequently, the reversal potential, $E_K$, may be effectively increased due to accumulation of K ions in the space between the axolemma and the external barriers (Frankenhauser and Hodgkin, 1956; Adelman et al., 1973). This mechanism can account for results such as those illustrated in Fig. 4. In this experiment (Clay, 1998), the membrane potential was held at −90 mV and stepped for 3 ms to the potentials indicated. The external solution was potassium ion free. Consequently, the deactivation (''tail'') current upon return to the holding level should be small and outward following all depolarizing steps, as predicted by the GHK equation. Indeed, the tail current following the step to −10 mV was outward, as shown more clearly by the inset (record **a**). The tail currents following depolarizations to 10, 30, and 50 mV were inward, which is consistent with accumulation of K ions in the extracellular space during the preceding depolarization. The increasingly large amplitude of the tail as the step potential was increased was due to both the accumulation effect and to an increase in activation of the conductance. During membrane depolarization $K_o$ rises from 0 to a finite level thereby producing a change in the shape of the *IV* curve and a change in current direction (Fig. 6). That is, when the membrane potential was stepped back to the holding level the tail current was inward, rather than outward. These results demonstrate that the $K^+$ concentration just outside the axolemma, referred to as $K_s$, is time-dependent during a voltage-clamp step. The model for the effect is

$$dK_s/dt = (\theta F)^{-1} I_K - (K_s - K_o)/\tau_1 - (K_s - K_o)/(\tau_2[1 + (K_s - K_o)/K_d]^3), \quad (6)$$

where $K_s$ and $K_o$ are the $K^+$ concentrations in the extracellular space and the bathing solution, respectively ($K_o = 0$ for the experiment in Fig. 4; $K_o = 10$ mM for seawater), $\theta$ is the width of the extracellular space (taken to be 12 nm), $F$ is the Faraday constant, and $\tau_1$ is the time constant of passive diffusion from the space ($\tau_1 = 12$ ms). The first two terms on the right-hand side of Eq. (6) are the predictions of standard diffusion theory (Adelman and Fitzhugh, 1975). The last term has been added to mimic the effect of a postulated uptake mechanism of K ions by the glial cell layer. The parameter $\tau_2$ is the apparent time constant of the effect ($\tau_2 = 0.2$ ms) and $K_d$ is its ''dissociation'' constant ($K_d = 2$ mM). Further details of the analysis are given in the legend of Fig. 4 and in Clay (1998). The accumulation/depletion process makes $E_K$ in Eq. (4) a time-dependent parameter. That is, $E_K(t) = 24 \ln(K_s(t)/K_1)$ where $K_s(t)$ is given by Eq. (6). With this modification, the mathematically reconstructed AP (Fig. 3E) is essentially indistinguishable from

the experimental recording in Fig. 3A and D. These results indicate that $K_s$ rises to approximately 16 mM during the latter part of the repolarization phase of the AP and immediately thereafter, which is 6 mM higher than the extracellular concentration ($K_o = 10$ mM).

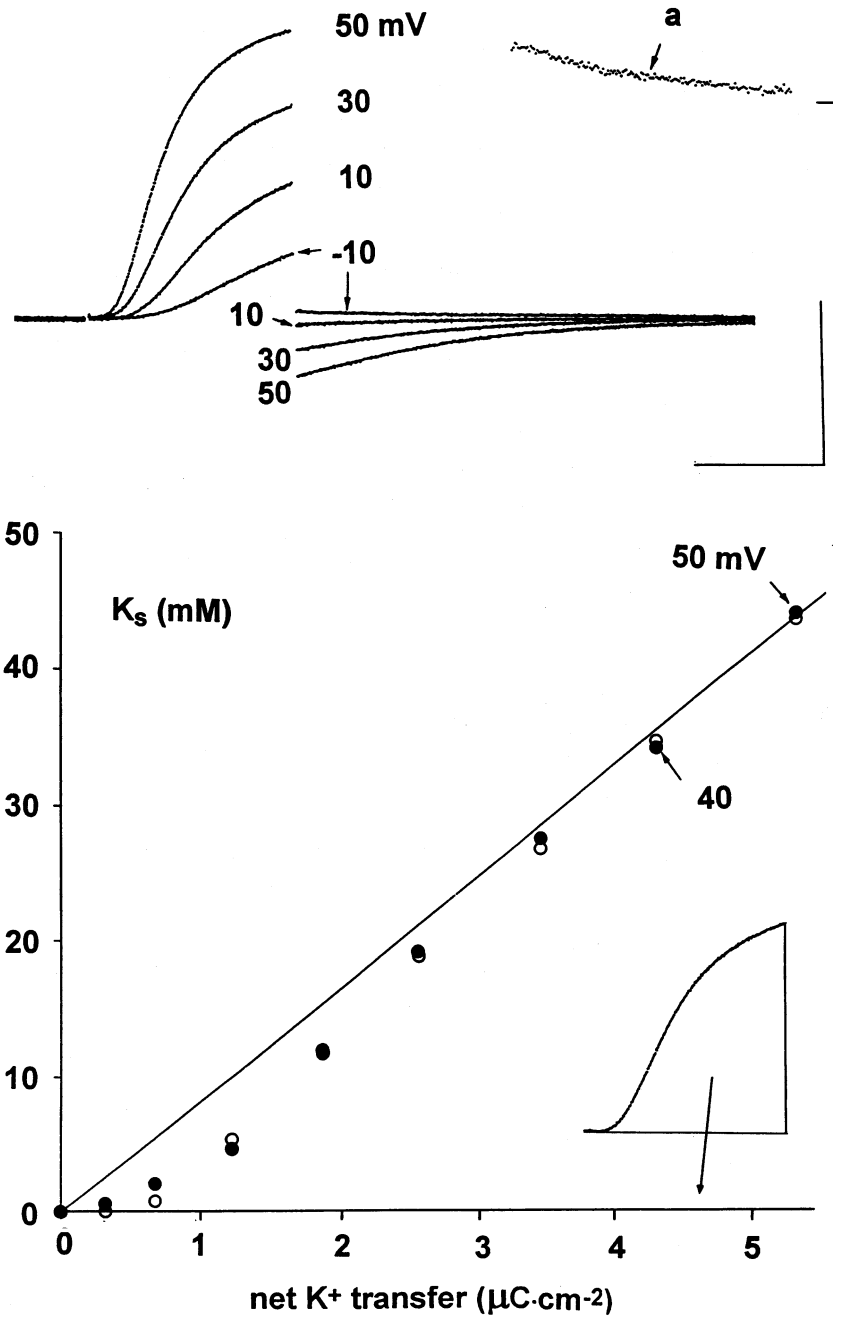

*2.1.5. Independent ion movements in $K^+$ channels?*

A key part of the above analysis is the observation that the voltage dependence of $K^+$ channel currents is consistent with the GHK equation. This result may seem surprising given that GHK was derived from macroscopic diffusion theory assuming independent movement of ions across the membrane (Goldman, 1943). In contrast, K ions are believed to move in a non-independent, coordinated, single-file manner through $K^+$ channels (Hodgkin and Keynes, 1955; Zhou et al., 2001; Berneche and Roux, 2001). The applicability of macroscopic diffusion theory to ion channels as well as the apparent paradox concerning independent ion movement can be elucidated by a specific type of single-file movement in which a channel contains at most a single vacancy (Schumaker and MacKinnon, 1990; Clay, 1991). The model consists of three sites that can be occupied by ions, consistent with recent crystallographic results on the bacterial KcsA $K^+$ channel (Zhou et al., 2001), and with the original tracer flux measurements of Hodgkin and Keynes (1955). The model has four states; one in which all sites are occupied by an ion and three in which a single site is vacant (Fig. 5). The sites are assumed to be symmetrically placed within the channel with the relative electrical distance of each site shown below the bottom right panel ($2d_1 + 2d_2 = 1$). Ions can enter or leave the pore from either side of the membrane with the constraint that only one site is vacant. Using algebraic manipulations, the flux $J_K$ through the channel is given by

$$J_K = a[\exp(-(2d_1 + d_2)V')([K^+]_i \exp(V') - [K^+]_o)//(\cosh(d_1 V')\exp(3d_2 V') + 2\cosh(d_2 V'))], \quad (7)$$

where $V' = V/24$, $a$ is a constant, and $\cosh x = (\exp(x) + \exp(-x))/2$. Fits of Eq. (7) and the GHK equation to $K^+$ current–voltage relations obtained with $300K_i^+/50K_o^+$ and $300K_i^+/300K_o^+$ are shown in Fig. 6 with $d_1 = 0.07$ and $d_2 = 0.18$. The single-file theory provides a remarkably close approximation to the GHK equation over the range of potentials used (−160–100 mV). Moreover, in the limit of an infinite number of equally spaced sites within the pore, the predicted flux is exactly equal to that given by GHK. The apparent paradox concerning the description of $K^+$ current–voltage relations by the GHK equation and the known multiple occupancy of $K^+$ channels is thereby resolved by a model in which ion vacancies move through the channel independently of each other. Further details of this analysis are given in Clay (1991). Hodgkin and

Fig. 4. $K^+$ accumulation in the restricted space outside the axon. Top panel: These currents were elicited with 3 ms duration voltage steps to the potentials indicated followed by a return to the holding level, −90 mV. The extracellular solution was $K^+$ free with TTX added to block $I_{Na}$. The GHK equation predicts outward tail currents following these steps, as was the case for the −10 mV result (also indicated by record **a** in the upper inset). The other three tail current records were inward due to accumulation of $K^+$ in the restricted space. That is, the accumulated $K^+$ causes the reversal potential to change from negative infinity with $K_o = 0$ to a levels above −90 mV thereby causing the tail current to be inward. The $K^+$ concentration in the restricted space at the end of each depolarizing step (labeled $K_s$) was determined from the currents at the end of the steps and at the beginning of each respective tail using the GHK equation. These results were plotted vs. the integral of the current during the depolarizing step (the charge transfer) in the bottom panel. The integration procedure is indicated in the lower inset. The straight line is the predicted level of $K_s$ if the only mechanism of removal of K ions from the space was passive diffusion. The calculated level (filled circles) was considerably below this predicted level for modest depolarizations, which suggest another mechanism for $K^+$ removal. An uptake mechanism was postulated, as described in the text. The predicted levels of $K_s$ with this model are indicated by the open circles. Further details are given in Clay (1998).

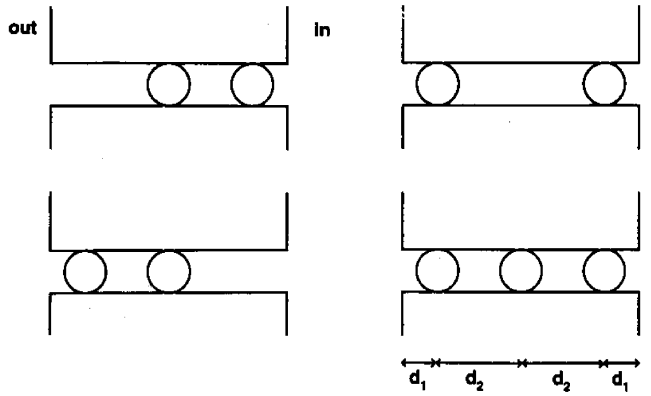


Fig. 5. Single vacancy model of single-file diffusion of potassium ions in $K^+$ channels. The model consists of three sites, only one of which is allowed to be vacant. All sites can be occupied. The model has four states. The electrical distances of each site are given below the right-hand panel. Further details are given in Clay (1991).

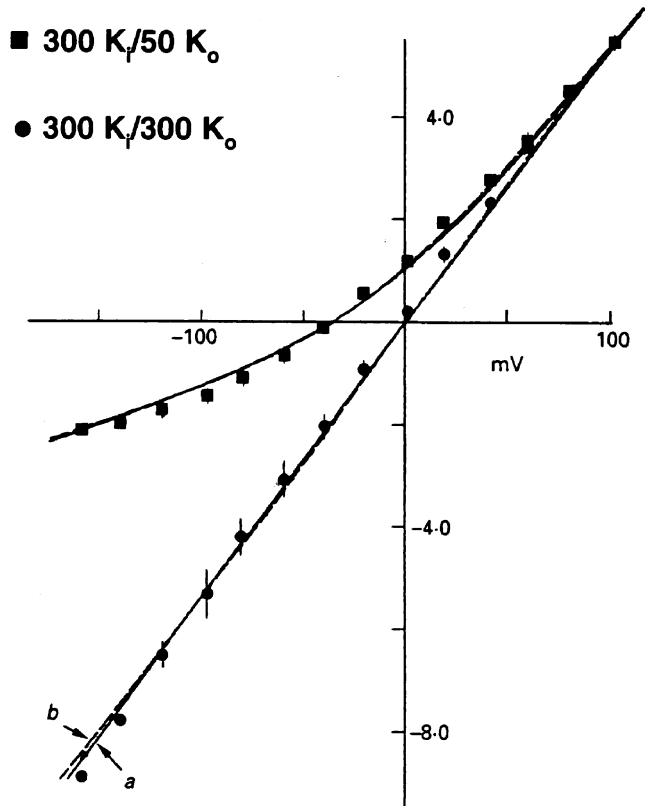


Fig. 6. Dependence of $K^+$ current on extracellular $K^+$ concentration. The data are described by the GHK equation (solid lines, as indicated by arrow ***a***) and the single vacancy model (dashed lines, as indicated by arrow ***b***). Further details are given in Clay (1991).

Keynes (1955) also considered vacancies in their original theory of single-file diffusion. They found that the theoretically determined value for the tracer flux ratio was reduced from $n+1$ to $n$, where $n$ is the number of binding sites in the channel, when occasional vacancies were allowed, so that their experimentally determined value of 2–3 for this ratio would correspond to 2–3 sites within the channel, rather than 1 or 2.

### 2.2. Potassium ion current, $I_K$—channel gating

The first demonstration of a discrepancy between the HH model and voltage-clamp recordings was the observation by Cole and Moore (1960) that the delay preceding the onset of $I_K$ activation following a depolarizing voltage step was significantly increased when a hyperpolarizing prepulse was used, moreso than predicted by the HH $n^4(V,t)$ model. They found that a model using $n^x(V,t)$ where $x=6$, or in some instances values of $x$ as high as 25, could provide a better description of their results than $x=4$. An AP with $x=6$ is shown in Fig. 7B along with the $x=4$ result in Fig. 7A. The $\alpha_n$ and $\beta_n$ parameters were shifted 5 mV in the hyperpolarizing direction so that $n^6_\infty(V)$ provided a fit to the $g_K$–$V$ results in Fig. 2 equivalent to that of $n^4_\infty(V)$ with the non-shifted $\alpha_n$ and $\beta_n$ (not shown). The AP with $n^6$ is virtually indistinguishable from the $n^4$ result. This analysis was extended to $n^{25}$ (Fig. 7C) with $\alpha_n = -0.01(V+80)/(\exp(-0.1(V+80))-1)$ and $\beta_n = 0.1\exp(-(V+85)/25)$ which provides a reasonably good fit of $n^{25}_\infty(V)$ to the $g_K - V$ curve, especially in the $-60$ to $-30$ mV range. The AP with $n^{25}$ is essentially the same as with either the $n^4$ or the $n^6$ description of $I_K$ gating. These results may be moot since the $n^x$ model has been ruled out as a mechanism at the molecular level by gating current measurements of heterologously expressed $K^+$ channels (Bezanilla et al., 1991; Taglialatela and Stefani, 1993). The ON gating current has a pronounced rising phase. The $n^x$ model implies $x$ independent gating particles, which predicts an instantaneous, outward jump in the gating current followed by an exponential decay to 0 regardless of the value of $x$ (Bezanilla et al., 1991; Clay, 1995). The Cole–Moore effect and the gating current results have prompted $K^+$ channel gating models of ever increasing

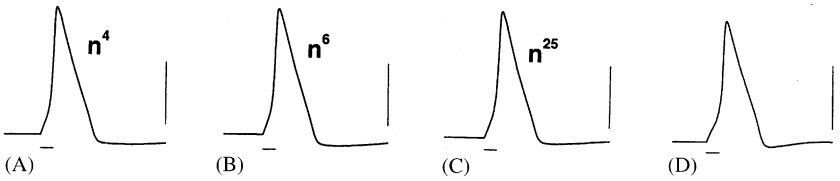


Fig. 7. Effects of the theoretical description of $I_K$ on the reconstructed AP. (A) Same result as in Fig. 3E. The $K^+$ channel current–voltage relation has the GHK dependence on driving force and accumulation/depletion is included. The $\beta_n$ term has been modified as described in the text, but the HH $n^4(V,t)$ model is otherwise unchanged. (B) Effect on the AP of using $n^6(V,t)$, in place of $n^4(V,t)$. Both $\alpha_n$ and $\beta_n$ were shifted 5 mV in the hyperpolarizing direction so that $n^6_\infty(V)$ gave a fit to the steady-state activation results in Fig. 2 that was equivalent to that of $n^4_\infty(V)$. (C) Similar result as in (B) using $n^{25}(V,t)$ in place of $n^4(V,t)$ with $\alpha_n = -0.01(V+80)/(\exp(-0.1(V+80)-1)$ and $\beta_n = 0.1\exp(-(V+85)/25)$. (D) Effect on the AP of using the Clay (1995) model of $I_K$ gating. The $n^x(V,t)$ term, where $x$ is either 4, 6, or 25, was replaced by $p_O(V,t)$, which is the solution to the coupled differential equations $dp_O(V,t)/dt = -\lambda_{23}p_1(V,t) - (\lambda_{23}+\lambda_{32})p_O(V,t)+\lambda_{23}$, $dp_1(V,t)/dt = -\lambda_{21} - (\lambda_{21}+\lambda_{12}(t))p_1(V,t) - \lambda_{21}p_O(V,t)$, and $d\lambda_{12}(t)/dt = -1.6(\lambda_{12}(t) - 2.2\exp(v/32))$, where $\lambda_{23} = 0.73\exp(V/50)$, $\lambda_{32} = 0.092\exp(-V/25)$, and $\lambda_{21} = 0.3\exp(-V/50)$. The calibrations are 1 ms and 50 mV, respectively. The top of the voltage bar corresponds to 0 mV.

complexity (Zagotta et al., 1994). An alternative approach, one in which the rate parameters between states in the model are time-dependent, can account for both results with a relatively small number of closed states (Clay, 1995). This model is given by $[C_1] \leftrightarrow [C_2] \leftrightarrow [O]$ in which [O] is the open state, $[C_1]$ and $[C_2]$ are closed states, and the forward rate parameter from $[C_1]$ to $[C_2]$ is time-dependent. The traditional approach with these models, including HH, is to assume that the rate parameters are strictly voltage-dependent. They change their values instantaneously following a voltage step. This assumption was relaxed in the Clay (1995) model. A similar approach was originally proposed by Hoyt (1982) to model the rising phase of $Na^+$ channel gating current. The AP using the Clay (1995) model was calculated by replacing $n^4(V, t)$ in Eq. (3) with $p_O[t]$, which is the probability that the $K^+$ channel is in its open state (further details are given in Fig. 7 legend and in Clay, 1995). The result (Fig. 7D) is not substantially different from the AP obtained with the $n^x$ model ($x = 4$, 6, or 25), except for the recovery phase. The point of this analysis is that excitability does not significantly depend upon the Cole–Moore effect nor does it appear to be influenced by a rising phase of the gating current. These effects are apparent only with relatively negative prepulse potentials that are well outside the range of potentials spanned by the AP.

### 2.3. Sodium ion current, $I_{Na}$

#### 2.3.1. Current–voltage relation

In their original work, HH assumed that $I_{Na}$—like $I_K$—was directly proportional to its driving force, $(V–E_{Na})$. Given that $K^+$ current is well described by the GHK dependence on driving force, one might reasonably ask if a similar conclusion applies to $Na^+$ current. The answer is yes, as shown by Vandenberg and Bezanilla (1991a). That is, $Na^+$ channels inwardly rectify since the intracellular $Na^+$ concentration is significantly less than the extracellular $Na^+$ concentration. However, $Na^+$ channels are blocked in an instantaneous, voltage-dependent manner by extracellular $Ca^+$ (Mozhayeva et al., 1982; Yamamoto et al., 1984; Vandenberg and Bezanilla, 1991a), so that the current–voltage relation is, serendipitously, a linear function of driving force, or nearly so, over the range of potentials spanned by the AP. Consequently, the $g_{Na}–V$ curve obtained by Hodgkin and Huxley (1952a) based on normalization of their peak $I_{Na}$ results by $(V–E_{Na})$ does not require revision, unlike the corresponding results for $I_K$. Similar results from squid giant axons following removal of inactivation by *N*-bromoacetamide (Oxford, 1981) are shown in the bottom panel of Fig. 2 along with the original $m^3_\infty$ curve from the HH model. This curve has a steepness similar to that of the revised $n^4_\infty$ model (Fig. 2, middle panel) with a midpoint that is approximately 15 mV positive to that of the $g_K–V$ result.

#### 2.3.2. Revisions in $I_{Na}$ gating

Kinetic results from neuronal $Na^+$ channels other than the activation curve are not well described by the HH model (reviewed by Patlak, 1991). In particular, activation appears to precede inactivation. That is, $Na^+$ channels first open and then inactivate following a voltage step. In the HH model inactivation is independent of activation. These and other aspects of squid $Na^+$ gating (macroscopic currents, single channel currents, and gating currents) are well described

by the following model (Vandenberg and Bezanilla, 1991b):

$$\begin{array}{ccccccccc} & & & & & \overset{a}{\underset{b}{\rightleftharpoons}} & & \overset{c}{\underset{d}{\rightleftharpoons}} & \\ & & & & [I_4] & & [I_5] & & [I] \\ & & & g \uparrow\downarrow j & & & & & f \uparrow\downarrow i \\ & \overset{y}{\underset{z}{\rightleftharpoons}} & & \overset{y}{\underset{z}{\rightleftharpoons}} & & \overset{y}{\underset{z}{\rightleftharpoons}} & & \overset{a}{\underset{b}{\rightleftharpoons}} & \\ [C_1] & & [C_2] & & [C_3] & & [C_4] & & [C_5] \end{array} \quad \overset{c}{\underset{d}{\rightleftharpoons}} \quad [O]$$

where $C_i (1 = 1, \ldots, 5)$ are closed states, $I_4$, $I_5$, and $I$ are inactivated states, and O is the open state, with the various voltage-dependent parameters, $a, b, c, d, g, j, f, i, y$, and $z$ given in Appendix A. Activation and inactivation are linked in this model, since the states $I_4$ and $I$ can be reached only from $C_4$ and O, respectively. The latter transition (i.e., the channel first opens) is the dominant pathway by which inactivation occurs (Bezanilla and Armstrong, 1977; Armstrong and Bezanilla, 1977). The $I_{Na}$ component in this scheme is given by (Clay, 1998)

$$I_{Na} = \frac{g'_{Na} V p_O (\exp((V - E_{Na})/24) - 1)}{[(\exp(V/24) - 1)(1 + 0.4\exp(-0.38V/24))]}, \tag{8}$$

where $p_O$ is the probability that the $Na^+$ channel is in its open state. Relatively little information has been provided concerning what may be the most important parameter in this model, namely $g'_{Na}$. Most studies of $I_{Na}$ gating subsequent to HH employed a relatively low concentration of extracellular sodium ions, $Na_o$, typically $\frac{1}{4}Na_o$, so as to minimize series resistance errors (Bezanilla and Armstrong, 1977; Kimura and Meves, 1979; Oxford, 1981). A representative recording from this work (Fig. 1, Oxford, 1981) has a peak inward current amplitude of 0.75 mA/cm$^2$ for a voltage step to 0 mV from a holding potential of −80 mV ($T = 6°C$). The value of $g'_{Na}$ in the Vandenberg and Bezanilla (1991b) model which matches this result is 180 mS/cm$^2$ ($\frac{1}{4}Na_o \rightarrow E_{Na} = 20$ mV), which, in turn, gives a peak inward current amplitude of 1.3 mA/cm$^2$ with $E_{Na} = 55$ mV. A similar result is obtained in the HH model if $g'_{Na}$ is reduced from 120 to 65 mS/cm$^2$.

### 2.3.3. *Effects of revisions in $I_{Na}$ on the action potential—threshold results*

The effects of the various descriptions of $I_{Na}$ (Vandenberg and Bezanilla, 1991b, HH, and HH with $g'_{Na}$ reduced) on the mathematically reconstructed AP are illustrated for near threshold responses in Fig. 8B–D, along with corresponding experimental results in Fig. 8A. The model of $I_K$ for this analysis was the same in Fig. 8B–D, which was also the same model of $I_K$ used in Figs. 3E and 7A–D. The experimental results (Fig. 8A) demonstrate a lack of an all-or-none character to the AP. The response is graded. Indeed, nerve membranes, at least those of squid giant axons, do not fundamentally have a threshold (Cole et al., 1970). The peak amplitude of the voltage response to a brief duration current pulse is a continuous function of pulse amplitude, although the range of amplitudes over which these results occurred is very narrow, so that, as a practical matter, a threshold does exist. Nevertheless, the amplitudes of both the subthreshold and suprathreshold waveforms are not given by a single number. In particular, the overshoot of the APs varied between +20 and 45 mV. A similar result occurred in the simulations in Fig. 8B and C. Graded responses are not as readily apparent with the original HH model of $I_{Na}$ ($g'_{Na} = 120$ mS/cm$^2$, Fig. 8D). Extremely fine changes in pulse amplitude are required to see the

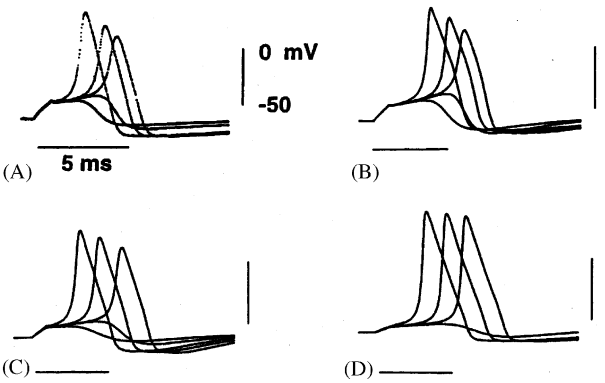


Fig. 8. Responses to near threshold stimuli. (A) Superimposed experimental results from a squid giant axon in response to 1 ms duration current pulses. The amplitudes of the pulses were all within 0.2 of 15 $\mu A/cm^2$. (B) Responses of the revised model with the Vandenberg and Bezanilla (1991b) description of $I_{Na}$. Pulse amplitudes were 14.9, 14.96, 14.967, 14.99, and 15.3 $\mu A/cm^2$. (C) Responses of the revised model with the HH description of $I_{Na}$ but with $g'_{Na}$ reduced from 120 to 65 $mS/cm^2$. Pulse amplitudes were 9.5, 9.83, 9.85, 10, and 11 $\mu A/cm^2$. (D) Same as in (C) but with $g'_{Na} = 120\,mS/cm^2$. Pulse amplitudes were 4.5, 4.75, 5, and 6 $\mu A/cm^2$. The same model of $I_K$ was used in (B)–(D), as described in the text.

continuous nature of the response (Fitzhugh and Antosiewicz, 1959; Clay, 1977). Indeed one could conclude, mistakenly, that the AP in the original HH model was all-or-none (Cole et al., 1955). However, their model lacks a saddle point threshold, which means that the excitatory response is, necessarily, a continuous function of the stimulus amplitude, albeit a very steep one in the transition between sub- and suprathreshold responses (Fitzhugh, 1955; Fitzhugh and Antosiewicz, 1959; Clay, 1977).

One conclusion from the results in Fig. 8 is that the modern view of $I_{Na}$ gating, in particular the observation that the gate opens before inactivation occurs, does not appear to be a significant factor for excitability. Additionally, the repolarization phase of the AP in the simulations with the Vandenberg and Bezanilla (VB) description of $I_{Na}$ (Fig. 8B) has a convex shape which is not apparent either in the experimental recordings (Fig. 8A) or in the model with the revised $I_K$ and the HH model of $I_{Na}$ having a reduced level of $g'_{Na}$ (Fig. 8C). The latter provides a better description of the experimental records than the VB model except for a discrepancy in threshold which is attributable to a larger amplitude of peak $I_{Na}$ for modest depolarizations ($V \sim -40\,mV$) compared to HH even with reduced $g'_{Na}$ in their model. A modification of the HH $\alpha_m$ and $\beta_m$ parameters may account for this discrepancy.

### *2.3.4. Responses to long duration current pulses*

A further test of models of excitability is their response to long duration current pulses. A characteristic feature of HH is repetitive firing during a sustained depolarizing current pulse (Rinzel, 1978). Similar behavior occurs with the revised model of $I_K$ and the HH description of $I_{Na}$ (Fig. 9C). In contrast, the axon itself fires once and only once under these conditions regardless of pulse amplitude or duration (Clay, 1998), which is consistent with the role it plays in squid behavior. It fires only once following a light flash (startle response) which is sufficient for contraction of the mantle (jet-propelled escape, Otis and Gilly, 1990). It fires once or twice

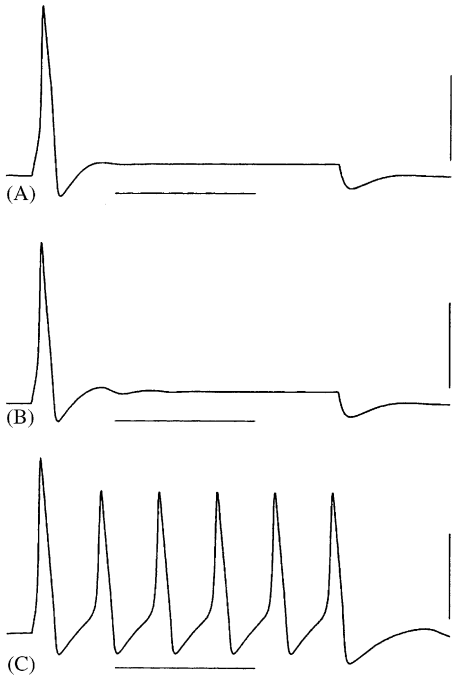


Fig. 9. (A–C) Responses of the revised HH model to a long duration current pulse with the Vandenberg and Bezanilla (1991b) model of $I_{Na}$ (A), the HH model of $I_{Na}$ with $g'_{Na} = 65\,mS/cm^2$ (B), and the HH model of $I_{Na}$ with $g_{Na} = 120\,mS/cm^2$ (C). The vertical calibration represents 50 mV (0 at top, −50 mV at bottom). The horizontal bar represents 20 ms. Accumulation/depletion of $K^+$ in the extracellular space was not included in these simulations.

(sometimes three times or not at all) with a subsequent jet-propelled escape in response to a chemical stimulus (Otis and Gilly, 1990). In other words, the axon is a strongly phasic preparation. A long train of spikes (a tetanus) apparently does not occur in vivo. The revised model with either the VB or the HH model of $I_{Na}$ having reduced $g'_{Na}$ predicts a similar result (Fig. 9A or B, respectively).

The above results are not unique to squid giant axons. Some walking leg axons from crustaceans, the so-called type III axons, are also phasic. They fire typically once, or at most 2–3 times, in response to sustained depolarization (Hodgkin, 1948; Connor, 1975). These axons lack the transient, potassium ion current, $I_A$, found in type I and II axons (Connor, 1975), preparations that do fire repetitively in response to sustained depolarization. These results might suggest that $I_A$ itself is responsible for repetitive firing. However, $I_A$ is an outward component under physiological conditions. It can have a significant effect on firing rate (Connor and Stevens, 1971), but another component—an inward current—must be responsible for the repetitive firing.

### 2.4. Leak current, $I_L$

In addition to $I_K$ and $I_{Na}$, Hodgkin and Huxley (1952b) recognized the existence of other ionic current pathways in nerve membrane which they lumped together in a single component termed the leak current, $I_L$, a time-independent current which is evident in voltage-clamp records by an

instantaneous current jump immediately following a voltage step. Some of the individual elements of $I_L$ are a chloride current, $I_{Cl}$ (Inoue, 1985), a persistent, tetrodotoxin (TTX)-sensitive sodium current, $I_{NaP}$ (Rakowski et al., 2002; Clay, 2003a), and a non-selective cation current activated by intracellular protons (Clay and Shrier, 2001). Additionally, squid giant axons also have a sodium–potassium pump (Rakowski et al., 1989) and a sodium–calcium exchanger (DiPolo and Beauge, 2002). Neither of these components appear to have significant effects for squid axon physiology. In particular, the pump has only minor effects on AP parameters (DeWeer and Geduldig, 1978). The exchanger does have a clear physiological role in various organs, including the heart, kidney, and brain (Blaustein and Lederer, 1999), but its effects in the brain are most significant at synapses, whereas its role in axonal physiology, if any, is unclear. Consequently, the focus here is on $I_{Cl}$, $I_{NaP}$, and the proton activated, non-selective cation current.

### 2.4.1. *Chloride ion current, $I_{Cl}$*

The chloride ion concentration in seawater is substantially higher than it is in axoplasm. Since this ion has negative charge, its inward movement across the membrane produces outward current over the range of potentials spanned by the AP, although its role during repolarization is minor relative to that of $I_K$ (Clay and Shrier, 2002). It is significant in setting the rest potential (Clay, 1988). Moreover, $I_{Cl}$, like $I_K$ and $I_{Na}$, is also well described by the GHK equation (Inoue, 1985). The model of this component in the simulations described below is given by (Clay and Shrier, 2002)

$$I_{Cl} = 0.6V(\exp(V/24) - 0.02)/(\exp(V/24) - 1)\,\mu A/cm^2. \quad (9)$$

### 2.4.2. *Persistent sodium ion current, $I_{NaP}$*

Squid giant axons have a TTX-sensitive, persistent (time-independent) sodium ion current, $I_{NaP}$ (Rakowski et al., 2002; Clay, 2003a). A similar current has been found in repetitively firing neurons in the mammalian brain (Crill, 1996). In squid axons $I_{NaP}$ has a threshold of $\sim -90$ mV and a maximal amplitude of $\sim 5\,\mu A/cm^2$ at $-50$ mV (Fig. 10). Its amplitude is reduced as the membrane potential approaches $E_{Na}$, consistent with it being $Na^+$ selective, as Rakowski et al.

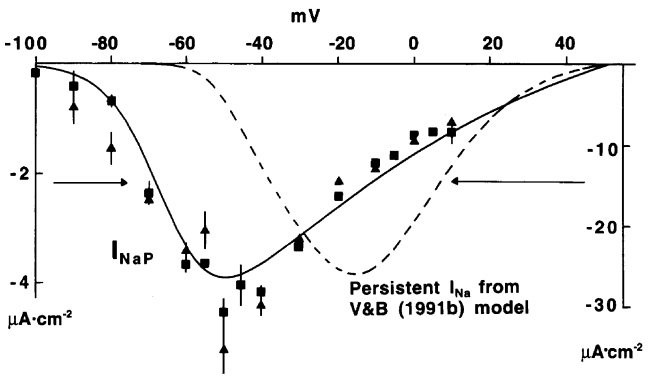


Fig. 10. Measurements of the persistent sodium current, $I_{NaP}$ (Rakowski et al., 2002; Clay, 2003a). The dashed line is the sustained current predicted by the Vandenberg and Bezanilla (1991b) model. The solid line is given by Eq. (10) in the text.

(2002) have demonstrated. It also is blocked by TTX, which suggests that it may be attributable to the classic $I_{Na}$ channel. Indeed, HH predicts a sustained current, the so-called "window" current (Attwell et al., 1979) attributable to the overlap on the voltage axis of the steady-state inactivation curve, $h_\infty(V)$, and $m^3_\infty(V)$. As noted above, the VB model provides a more complete description of $I_{Na}$ results than does HH. It also predicts a persistent current (Fig. 10), which does not adequately describe the $I_{NaP}$ results. Specifically, the persistent current in the VB model has a threshold of −60 mV, rather than −90 mV, with a peak amplitude of ~30 μA/cm$^2$ at −15 mV, significantly larger than the value of 5 μA/cm$^2$ at −50 mV in the measurements of $I_{NaP}$. One factor missing from this analysis is slow inactivation of the $I_{Na}$ channel (Rudy, 1978; Clay, 2003a). The time constant of this gating mechanism is several seconds (top panel, Fig. 11). It first becomes clearly apparent at −70 mV (bottom panel, Fig. 11). A convenient way of determining its voltage dependence in steady state is by holding the membrane potential at various levels between −100 and −30 mV for several minutes and then stepping to a test potential of 0 mV to elicit the remaining $I_{Na}$. These results demonstrate that inactivation is complete at −40 mV (Fig. 11). Moreover, the true steady-state inactivation curve is steeper than the "classical" inactivation curve, and its midpoint is shifted leftward on the voltage axis. When the slow process is taken into account, the persistent current predicted by the VB model is relatively small, and constrained to the −60 to −40 mV range (Fig. 12). This current has been subtracted from the $I_{NaP}$ results in Fig. 10 to give that portion of $I_{NaP}$, the major portion, which is attributable to an $Na^+$ channel distinct from $I_{Na}$ (Clay, 2003a). The solid line describing this result is given by

$$I_{NaP} = \frac{6(V/24)(0.03\exp(V/24) - 0.43)}{[(\exp(V/24) - 1)(1 + \exp(-(V + 65)/7))]}\,\mu A/cm^2. \quad (10)$$

The $I_{NaP}$ component does not have a clear role in membrane excitability for physiological conditions. When the intracellular pH ($pH_i$) is increased above 7.8, it is responsible for spontaneous, repetitive activity, as described below.

### 2.4.3. Non-selective cation current

A non-selective cation channel activated by extracellular protons has been found in sensory neurons of dorsal root ganglion cells (Bevan and Yeats, 1991). This channel is not voltage-gated. A similar channel appears to be present in squid giant axons, although the proton sensitivity is on the intracellular surface of the axolemma (Clay and Shrier, 2001). An increase in the $pH_i$ from a physiological level ($pH_i = 7.2$) to 8.5 caused a marked increase in membrane impedance (Fig. 13). This experiment was carried out with TTX in the external solution to block both $I_{Na}$ and $I_{NaP}$. A hyperpolarizing current pulse with $pH_i = 7.2$ produced a response corresponding to an input resistance of 0.7 kΩ/cm$^2$ and a time constant of 0.7 ms (Fig. 13A). Both results are consistent with the small signal impedance measurements of Hodgkin and Huxley (1952d). The response to the same amplitude current pulse with $pH_i = 8.5$ had a much greater amplitude and a significantly longer time course (Fig. 13A). Indeed, the response had not yet reached steady state at the end of 10 ms. The increase in membrane resistance and the relatively long time constant of the response are both consistent with the virtual absence of membrane current in the −59 to −93 mV voltage range. The $I_{NaP}$ component was blocked by TTX. Moreover, the intracellular perfusate in this experiment did not contain chloride ions (Clay and Shrier, 2001). Consequently, $I_{Cl}$ was virtually absent in the −59 to −93 mV range. Furthermore, $I_K$ was also virtually absent, since this potential

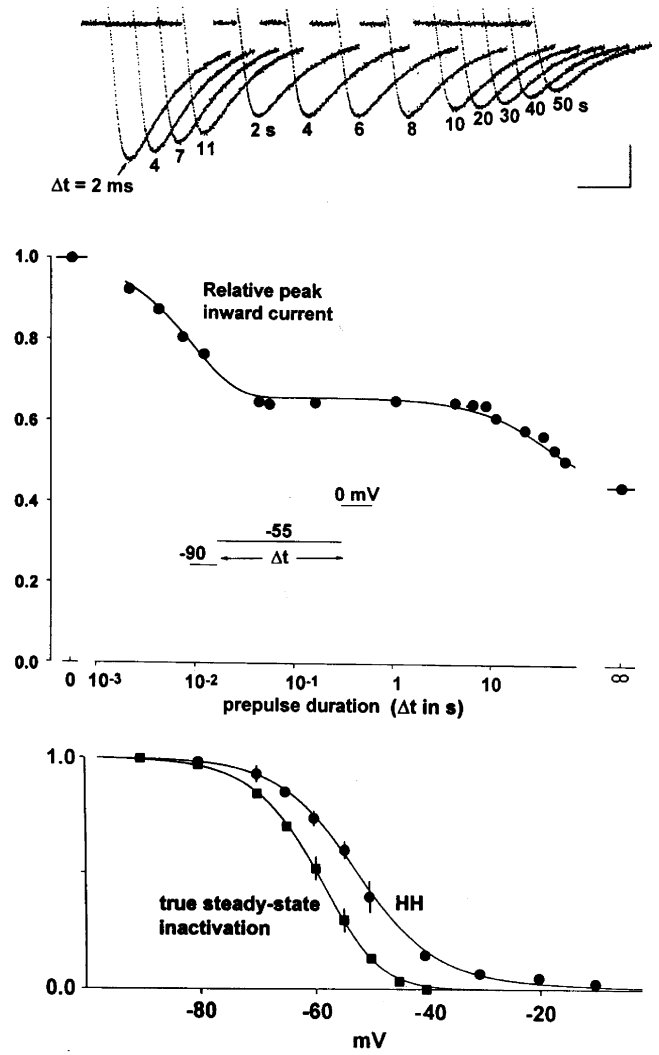


Fig. 11. Slow inactivation of $I_{Na}$. Top panel: Measurements of $I_{Na}$ elicited by a 7 ms step to 0 mV following a prepulse to −55 mV for the times indicated alongside each record. (The $I_K$ component was blocked by perfusing the axon with a solution in which $K^+$ was replaced by $Cs^+$.) The calibrations represent 3 ms and 0.25 mA/cm$^2$. Middle panel: Peak $I_{Na}$ as a function of prepulse duration (logarithmic scale). Bottom panel: Steady-state inactivation obtained with a 50 ms duration pulse (results labeled HH) and by holding the membrane potential at the levels indicated on the abscissa for 5 min (true steady-state inactivation). Further details given in the text and in Clay (2003a).

range is below threshold of activation of $I_K$. These results are consistent with the presence of a single current component in the subthreshold voltage range with $pH_i = 7.2$, a component which is absent, or nearly so, with $pH_i = 8.5$ (Fig. 13B). In other words, it is activated by intracellular protons and is likely permeant to both $Na^+$ and $K^+$. Moreover, it is significant for physiological conditions, since it depolarizes the membrane potential from the foot of the AP to the resting potential. The absence of this current with elevated $pH_i$ is a critical factor that leads to

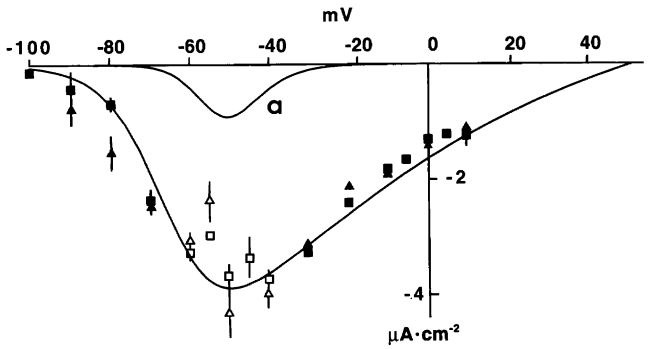


Fig. 12. Analysis of the $I_{NaP}$ results given in the text and in Clay (2003a). The curve labeled **a** represents the predicted steady-state current of the VB model.

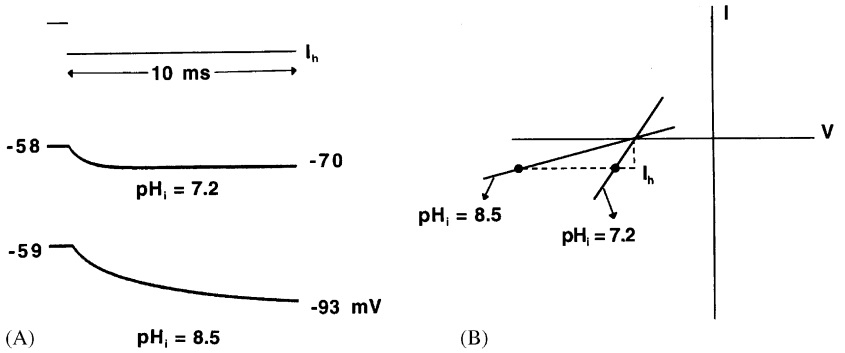


Fig. 13. Change in impedance produced by elevated $pH_i$. (A) The top panel illustrates a step in current which elicited the voltage responses shown below with physiological $pH_i$, 7.2 and $pH_i = 8.5$. The non-selective cation current was substantially reduced by alkaline $pH_i$ as indicated schematically in (B). Consequently, the current pulse produced a large voltage change with a significantly increased time constant of the response with alkaline pH.

spontaneous, repetitive firing (Clay and Shrier, 2002). This component is given by $g(V + 49)$, where $g = 0.3$ for physiological $pH_i$ and $g = 0$ for $pH_i > 7.7$.

## 3. Spontaneous firing with elevated intracellular pH

Traditionally, excitability of squid giant axons has been increased by lowering the extracellular calcium ion concentration (Huxley, 1959; Guttman and Barnhill, 1970). Work in this laboratory (J.R. Clay, unpublished results) has also shown that repetitive, or even autonomous activity in squid giant axons occurs for these conditions. However, the effect was transient and episodic. Moreover, axons became inexcitable 15–20 min following the change to low $Ca^{2+}$ seawater, which is not surprising given the known deleterious effect of low external $Ca^{2+}$ medium on neurons (Horn, 1999). A robust, long-lasting increase in excitability was observed (Fig. 14) following an increase in the $pH_i$ above 7.7 (Clay and Shrier, 2001, 2002). A current pulse applied with

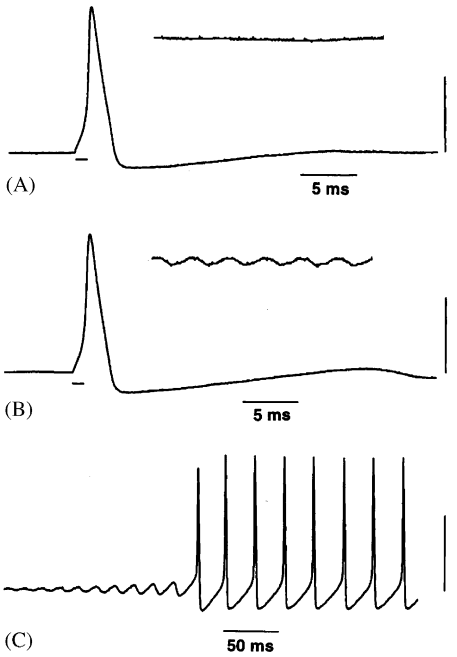


Fig. 14. Spontaneous firing of APs elicited by alkaline $pH_i$, as described in the text. (A) Response of an axon to a 1 ms duration 20 $\mu A/cm^2$ amplitude current pulse (indicated by the bar below the AP). The vertical bar to the right represents 50 mV (0 mV at the top of the bar). The inset is a recording of the rest potential on an expanded voltage scale and a reduced time scale (4 × in each case). (B) This recording was obtained 2 min following an increase of the $pH_i$ to 8.5. The voltage rebound following a current pulse was substantially increased, and spontaneous voltage fluctuations about the rest potential were observed (inset). Same calibrations as in (A). (C) This recording was obtained 1 min following the record in (B). The oscillations in the membrane potential slowly increased until an unending train of APs occurred. Further details are given in Clay and Shrier (2001).

physiological conditions ($pH_i = 7.3$, Boron and DeWeer, 1976) produced a typical AP response followed by a slight oscillatory rebound (Fig. 14A). The rebound was considerably larger 2 min after a change to an intracellular perfusate with pH of 8.5 (Fig. 14B). Moreover, the membrane potential oscillated around the rest level spontaneously (inset, Fig. 14B). About 1 min later, the oscillations increased in amplitude until AP threshold was crossed resulting in an unending train of APs. The activity lasted throughout the course of the experiment, which in one case was 4 h long. These preparations were perfused both inside and out so that rundown of the ionic gradients during such long recordings was not a factor. The effect was reversible and it appeared to have a threshold at $pH_i \sim 7.7$ (Clay and Shrier, 2001). No clear changes in the either the frequency of spontaneous firing or in the shape of the voltage waveforms was observed for $pH_i > 7.7$ up to $pH_i = 9$. The physiological relevance of these results for squid behavior, if any, is unknown (Clay and Shrier, 2001).

The ionic mechanisms underlying automaticity with elevated $pH_i$ are subtle. No clear effect of a change in $pH_i$ on $I_{Na}$ in the 7–9 range was observed. An irreversible reduction of $I_{Na}$ does occur for $pH_i > 9.5$ (Brodwick and Eaton, 1978), which is outside of the range of $pH_i$ used in Clay and Shrier (2001, 2002). Moreover, a reversible blockade of $I_{Na}$ by intracellular protons has been

reported having $pK_a$ values of 4.6 and 5.8 (Wanke et al., 1980a), which is also outside of the range of $pH_i$ used in these experiments. Changes in $pH_i$ in the 7–9 range do have effects on $I_K$ (Wanke et al., 1980b; Clay, 1990). Specifically, slow inactivation of $I_K$ is altered—C-type inactivation—(Ehrenstein and Gilbert, 1966; Clay, 1989). In the steady state approximately 15% of the conductance is slow-inactivated at −60 mV. The effect of increasing $pH_i$ above its physiological level of 7.3 is to shift the inactivation curve rightward on the voltage axis, thereby increasing by 15% the amount of $K^+$ conductance available for activation during an AP. This effect is too small and in the wrong direction to explain an increase in excitability. The only remaining element of the Hodgkin and Huxley (1952d) model is the leak current, which as noted above consists of $I_{Cl}$, $I_{NaP}$, and a proton activated cation conductance. The latter is removed with elevated $pH_i$, leaving primarily $I_{NaP}$ in the subthreshold voltage range. This current provides a sufficient mechanism for the $pH_i$-induced automaticity. Specifically, it destabilizes the resting state, thereby causing spontaneous firing (Fig. 15, taken from Clay and Shrier, 2002). With elevated $pH_i$ the steady-state current–voltage ($IV$) relation has negative slope for potentials below −62 mV, which is attributable to $I_{NaP}$. The $IV$ has positive slope where it crosses the voltage axis, but this point is unstable. A slight perturbation away from this point causes subthreshold oscillations in the membrane potential which ultimately grow in amplitude until AP threshold is crossed, resulting in an unending train of AP's results, very much like the experimental record in Fig. 14. Further details are provided in Clay and Shrier (2002).

## 4. Simplified models of excitability

Because of the complexity of the HH equations, several attempts have been made to devise simplified models that retain the basic features of axonal excitability. Perhaps the most notable of these is the Fitzhugh and Nagumo (FN) model (Fitzhugh, 1961; Nagumo et al., 1962), given by

$$\begin{aligned} dV/dt &= -V(V-1)(V-a) - W - I_{stim}, \\ dW/dt &= c(V - bW), \end{aligned} \tag{11}$$

where $V$ corresponds to the membrane potential (dimensionless), $W$ is a recovery, or refractory, parameter, $a = 0.14$, $b = 2.4$, and $c = 0.008$, and $I_{stim}$ is the stimulus current. The model does not have a term corresponding to ionic current. Nevertheless, it has non-linear features that mimic membrane excitability. In particular, an AP waveform is elicited and this response is graded (Clay and Shrier, 1999). An additional qualitative similarity between behavior of squid giant axons and the FN model concerns responses to a repetitive train of brief duration current pulses (Fig. 16). Experimentally, only the first pulse elicited an AP (Fig. 16A). All of the subsequent pulses elicited a subthreshold response even though the amplitude of the pulses was the same as the first. Similar results were obtained over a relatively broad range of pulse amplitude and pulse frequency conditions, although APs were observed intermittently with this protocol with either a sufficiently low pulse frequency, or sufficiently high pulse amplitude (Kaplan et al., 1996). The HH model exhibited an alternating pattern of an AP and a subthreshold waveform with a protocol similar to that used experimentally (Fig. 16B). That is, an AP is not elicited in response to a second current pulse for a period of time following an AP elicited by an initial current pulse—the refractory period originally described by Hodgkin and Huxley (1952d). The results in Fig. 16A demonstrate

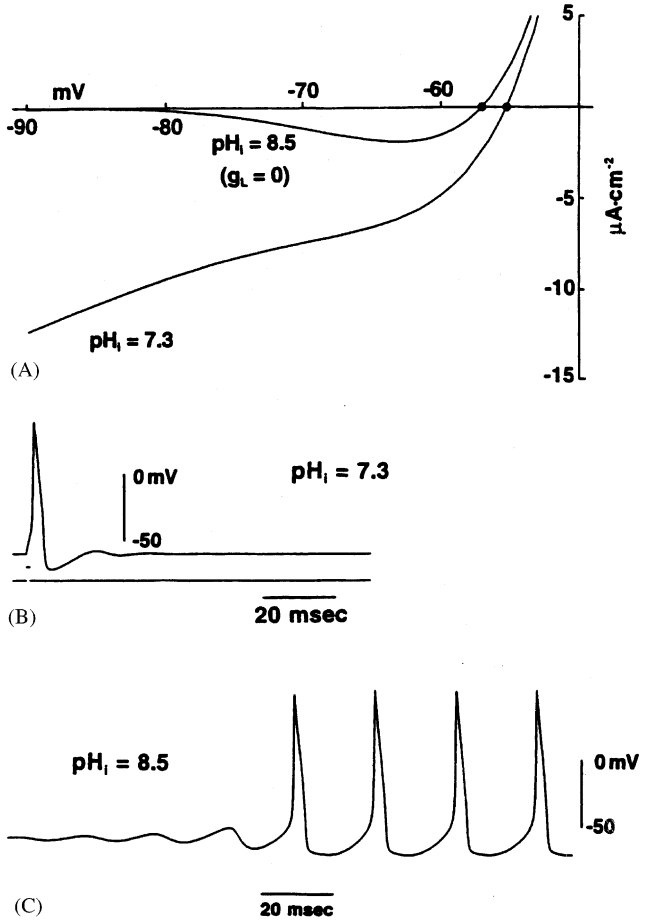


Fig. 15. (A) Steady-state current–voltage relations (*IV*'s) in the Clay (1998) model revised to account for the effects of alkaline $pH_i$ on excitability (Clay and Shrier, 2002). With $pH_i = 8.5$ the *IV* has negative slope for potentials below $\sim -62$ mV, which is attributable to the persistent sodium current, $I_{NaP}$. The model is stable for $pH_i = 7.3$. A brief duration current pulse elicited an AP (B) followed by a return of the membrane potential to rest level. The model fired only once even with a sustained current pulse (not shown). The model is unstable for $pH_i = 8.5$. A slight perturbation from the voltage at which net current is zero, in the steady state, resulted in spontaneous subthreshold oscillations, which grew in amplitude until AP threshold was reached. The model then fired in a stable, repetitive manner (C). Additional details are given in Clay and Shrier (2002).

that the axon is even more refractory than the HH model. Similar behavior cannot be readily mimicked in the revised HH model even with reduced $g'_{Na}$ (simulations not shown). It is mimicked with the VB description of $I_{Na}$ and the revised version of $I_K$ (Clay, 1998, Fig. 4) and, qualitatively, by the FN model (Fig. 16C). These results further illustrate the point made previously, which is that the HH model is too excitatory. In this instance simply reducing $g'_{Na}$ is not sufficient to eliminate, or reduce the discrepancy between the model and experiment. The FN model exhibits refractory properties similar to the experimental recording, but this comparison is disconcerting since the AP duration of the model is significantly greater than that of neuronal APs. The AP

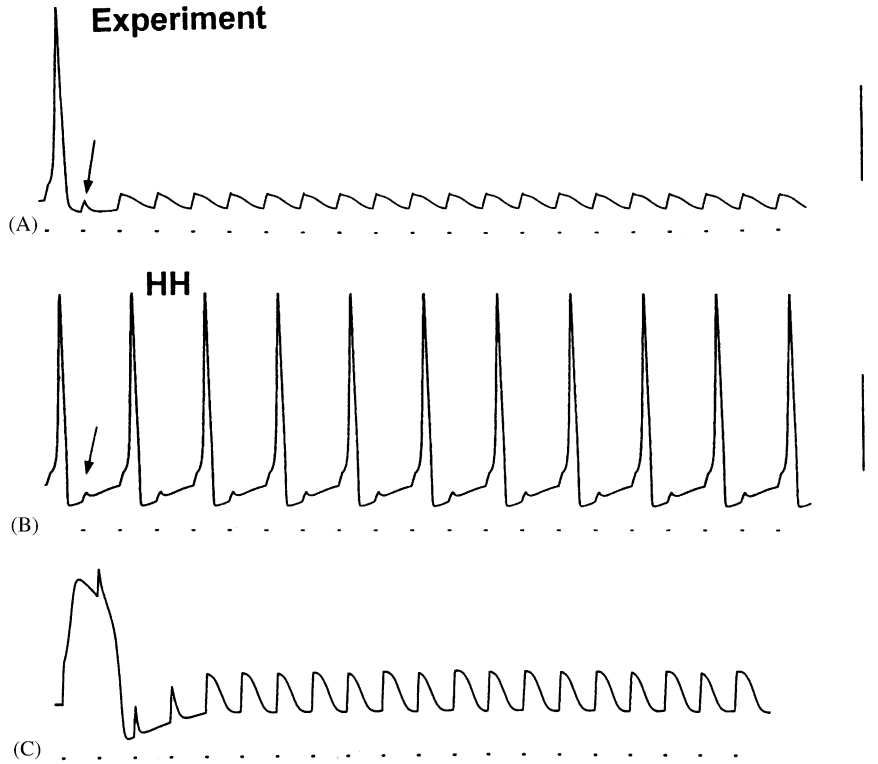


Fig. 16. Responses to a train of brief duration current pulses. (A) Voltage recording from an axon stimulated by 1 ms pulses at 105 Hz. Pulse amplitude was 17 mA/cm$^2$. The first pulse elicited an AP but none of the others did. (B) Response of the HH model to the same stimulus protocol with 8 mA/cm$^2$ pulses. The times of pulse application in both (A) and (B) are indicated below each respective recording. (C) Response of the Fitzhugh–Nagumo model (FN) to a train of near threshold current pulses. The time between pulses was 23 units in the FN model. Pulse amplitude was 0.22.

duration of a related model by Hindmarsh and Rose (1982) is similar to that of axons. This model predicts repetitive firing have a frequency–stimulus relation similar to that of snail neurons and some crustacean axons (type II).

## 5. Role of noise in axonal excitability

An underlying assumption of the results described to this point is that membrane current is a continuous function of time during a voltage-clamp step and that membrane voltage responses to a current stimulus are regular. That is, the response to a given stimulus is the same for each application of the stimulus. Blair and Erlanger (1932) and Monnier and Jasper (1932) found the latter not to be the case for single myelinated axons. Specifically, an AP was not always elicited in response to a near threshold current pulse. Similarly, the near threshold responses in Fig. 8A of this study were also variable. In particular, the same graded response was not elicited each time by the same amplitude current pulse (results not shown). The variability must be attributable to noise from some source, as described below.

### 5.1. Membrane noise

During the 60s and 70s a number of studies on various axon preparations demonstrated the existence of a significant excess current noise (Poussart, 1971; Conti et al., 1975, 1976; and references contained therein). Those results were later shown to be attributable to random, spontaneous openings and closings of individual $I_K$ and $I_{Na}$ channels (Conti and Neher, 1980; Sigworth and Neher, 1980). Lecar and Nossal (1971a, b) attributed the fluctuations in excitability at the node of Ranvier observed by Blair and Erlanger (1932) and Monnier and Jasper (1932) to $Na^+$ current noise, an observation later confirmed by Sigworth (1980). In particular, the number of $Na^+$ channels in a single node, $N \sim 7.5 \times 10^4$, is consistent with the observed degree of fluctuations in excitability based on the theoretical analysis of Lecar and Nossal (1971a, b). The relative spread of the fluctuations, $R = \sigma/S$, where $\sigma$ is the standard deviation of the threshold and $S$ is the threshold stimulus, is approximately 1% (Sigworth, 1980). Application of this analysis to squid axons can be made with the knowledge that the recordings were obtained from a 1 mm length of axon electrically isolated from 5 mm of axon on either side (Fig. 1, Adelman and Palti, 1969). The number of $Na^+$ channels in this central region is $\sim 5 \times 10^8$ for a 500 μm diameter axon (representative for these experiments) with 300$Na^+$ channels/μm$^2$ (Conti et al., 1975), which is four orders of magnitude more than in a node of Ranvier. Fluctuations in excitability are believed to be proportional to $1/\sqrt{N}$ (Lecar and Nossal, 1971a, b). Based on this analysis, $R =$ 0.01% for threshold fluctuations in squid axons, an undetectable level. In other words, squid giant axons are too large for current noise to have a significant effect on membrane excitability. The extreme regularity of spontaneous firing with elevated $pH_i$ (Fig. 14C and other results not shown) is consistent with this observation. The simulations in Fig. 8, which were noise-free, demonstrate that a change in stimulus amplitude by 1 part in $10^3$ at the steepest portion of the stimulus–response curve, which is within the noise range of the stimulator, is sufficient to significantly alter the response. Consequently, the variability of those responses to repeated threshold stimuli is likely due to equipment noise. Nevertheless, random openings and closings of individual channels can have a significant effect on excitability in a membrane patch containing only a few channels (Clay and DeFelice, 1983). Channel noise may itself lead to spontaneous firing of APs in a small patch (Strassberg and DeFelice, 1993). Moreover, it may be a factor in spike timing in small axons (Schneidman et al., 1998; Steinmetz et al., 2000), although variability in synaptic input would appear to be a more significant factor (Reyes and Fetz, 1993a, b).

### 5.2. Irregular firing in the absence of noise

As noted above, irregular neuronal firing is generally attributed to variability in synaptic input, channel noise, or perhaps, both. A third possibility, namely irregular firing due to the non-linear dynamics of the underlying ion currents, has not received much attention. This mechanism is a direct outcome of graded APs. It is apparent both experimentally and theoretically using the periodic pulse protocol described in Fig. 16 (Kaplan et al., 1996). In this experiment each pulse, save for the first, elicited a subthreshold response (Fig. 16A). The pulse frequency was 105 Hz. When the frequency was reduced to 80–90 Hz, APs were occasionally elicited at irregular intervals (Kaplan et al., 1996). Similar results can be simulated in the FN model, namely irregular firing in the absence of noise, a result which is related to deterministic chaos (Kaplan et al., 1996;

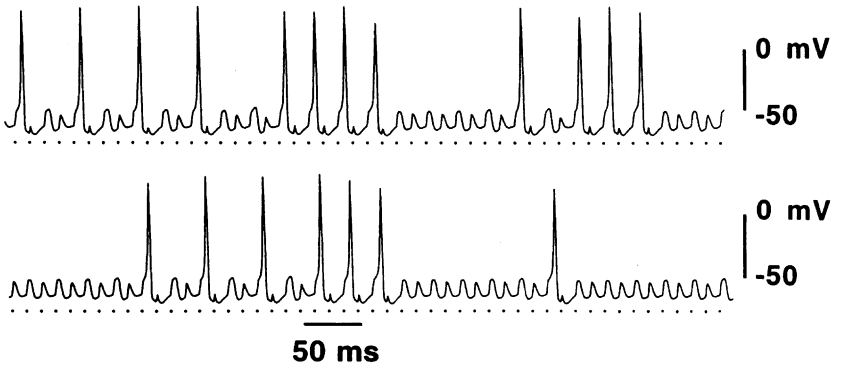


Fig. 17. Irregular firing in the revised HH model with the VB description of $I_{Na}$ and the revised description of $I_K$ given in the text. Taken from Clay (2003b).

Guckenheimer and Oliva, 2002). This result also occurred in the model with the VB $I_{Na}$ and the revised description of $I_K$ (Fig. 17, taken from Clay, 2003b). The APs do not have a fixed amplitude or duration. Consequently, the degree of $g_{Na}$ and $g_K$ activation at the end of any given spike is variable and that variability in turn determines the time the system remains in the subthreshold region prior to the next AP. If the APs were fixed events, as is the case with integrate and fire models (Gerstein and Mandelbrot, 1964; Tuckwell, 1988), no variability would occur in the absence of noise since the duration of the train of subthreshold responses is determined by the state of the model at the end of any given AP. In other words, variability in timing of spikes in the model is not determined by the subthreshold events just prior to an AP, but rather by the APs themselves. This effect is robust since the graded spikes have a broad range of amplitudes and durations (Clay, 2003b). The AP in the HH model even with reduced $g_{Na}$ is largely a stereotypical event except for a very narrow range of parameters (Guckenheimer and Oliva, 2002). The physiological significance of the irregular firing, if any, has not been determined (Clay, 2003b).

## 6. Myelinated axons

The other classic nerve membrane preparation in addition to squid giant axons is the amphibian node of Ranvier in myelinated axons. Significant advances from the former preparation were usually followed by similar advances in the latter. Two examples of this are the Frankenhauser and Huxley (1964) model of the AP, which was based on the original HH model, and the measurements of $Na^+$ channel gating current by Nonner et al. (1975), which closely followed the original gating current measurements of Armstrong and Bezanilla (1973). Mammalian myelinated axons, including those from humans, lack a significant voltage-gated $K^+$ current (Chiu et al., 1979; Schwarz et al., 1995). These results together with the observation of the transient potassium ion current in crustacean axons in addition to $I_K$ in those preparations (Connor, 1975) are consistent with the general theme that differences in the shape of electrical activity in different cell types, or in the same cell type from different animals, are attributable to differences in $K^+$ currents (Rudy, 1988). By contrast, $I_{Na}$ serves primarily to rapidly depolarize

the membrane potential to the vicinity of $E_{Na}$, a common requirement for most excitable cells. This observation may explain why $I_{Na}$ is widely conserved, moreso than $K^+$ currents, even for axons.

The shape of the AP in the absence of $I_K$ can be illustrated by the model of the human node of Ranvier of Schwarz et al. (1995), which is given by

$$dV/dt = -C^{-1}(I_{Na} + I_{Ks} + I_L + I_{stim}), \tag{12}$$

where $C = 1.4\,pF$, $I_{stim}$ is the stimulus, $I_L$, the leak current, is given by $30(V + 84)$, $I_{Ks}$, a relatively small, slowly activating $K^+$ current is given by $30s(V + 84)$ with $ds/dt = -(\alpha_s + \beta_s)s + \alpha_s$ where $\alpha_s = -0.00211(V+12.5)/(\exp(-(V+12.5)/23)-1)\,ms^{-1}$ and $\beta_s = 0.00128(V+80.1)/(\exp((V+80.1)/21.8) - 1)\,ms^{-1}$, and $I_{Na} = m^3hFP_{Na}(V/25.73)(Na_o - Na_i \exp(V/25.73))/(1 - \exp(V/25.73))$, with $dm/dt = -(\alpha_m + \beta_m)m + \alpha_m$, $dh/dt = -(\alpha_h + \beta_h)h + \alpha_h$, where $\alpha_m = -2.75(V+18.4)/(\exp(-(V + 18.4)/10.3) - 1)\,ms^{-1}$, $\beta_m = 0.127(V + 22.7)/(\exp((V + 22.7)/ 9.16) - 1)\,ms^{-1}$, $\alpha_h = 0.0571(V + 111)/(\exp((V + 111)/11) - 1)\,ms^{-1}$, $\beta_h = 3.91/ (\exp(-(V + 28.8)/13.4) + 1)\,ms^{-1}$, $F = 9.65 \times 10^4\,C/mol$, $P_{Na} = 3.52 \times 10^{-9}\,cm^3/s$, $Na_o = 154\,mM$, $Na_i = 35\,mM$, and $T = 25°C$. All currents are in pA, $V$ is in mV, and $t$ in ms. Three responses of the model to near threshold stimuli are shown superimposed in Fig. 18. The response is a continuous function of stimulus amplitude, although this relation is very steep in the vicinity of threshold. The rest potential in the model is $E_K$. Consequently, an undershoot does not occur and would not even if $I_K$ were included. The $I_{Ks}$ component is a factor in determining threshold, but not in the shape of the AP. The latter is determined by $I_{Na}$, in particular $I_{Na}$ inactivation, and the leak current.

## 7. Conclusions

The original formulations of $g_{Na}$ and $g_K$ by Hodgkin and Huxley (1952d) continue to be used to describe membrane excitability even though they do not adequately fit voltage-clamp

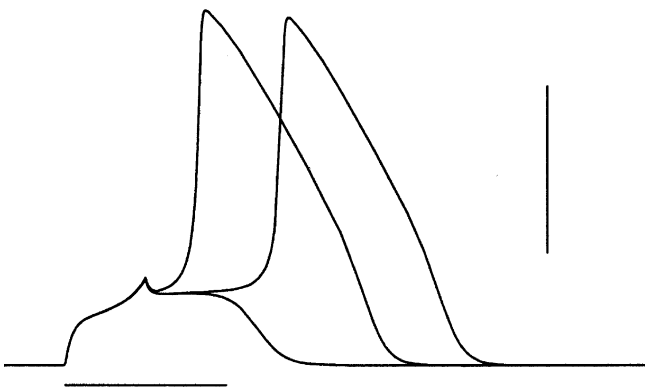

Fig. 18. Three near threshold voltage responses of the Schwarz et al. (1995) of the human node of Ranvier. The calibrations represent 1 ms and 50 mV, respectively.

measurements. The deviations between the $m^3h$ and $n^4$ models and corresponding results for $I_{Na}$ and $I_K$, respectively, do not appear to be significant for the action potential. Models that do describe those results are significantly more complex than the $m^3h$ and $n^4$ models, which limits their utility in computational neuroscience, especially since they seem not to be necessary. The shortcomings of the $m^3h$ and $n^4$ models suggest that they will not be useful for ion channel structure function relationships at the molecular level other than the observation that the choice of $n^x$ by HH with $x = 4$ rather than some other number such as three or five, which was obtained by empirically curve fitting this model to $K^+$ current traces, serendipitously foreshadowed by almost 50 years the finding that $K^+$ channels are homotetramers (Doyle et al., 1998). These models, in particular, the $m^3h$ model will also almost certainly be inadequate to describe $I_{Na}$ ''channelopathies'', which are inherited conditions, such as epilepsy, caused by mutations in genes encoding the $I_{Na}$ channel (Cannon, 2002). A consistent gating defect in these mutants is incomplete inactivation at depolarized potentials resulting in a persistent current, attributable to $I_{Na}$ not to $I_{NaP}$. The persistent current is approximately 1–4% of the transient peak inward current, which has a clear influence on excitability at the cellular level (Cannon, 2002; Lossin et al., 2002). Kinetic models that describe these results have recently been formulated (Clancy and Rudy, 1999).

Two other modifications in HH noted above concern the current–voltage relation for the $K^+$ channel and accumulation of $K^+$ in the extracellular space just outside the axolemma. Current through the $K^+$ channel has a voltage dependence that is well described by the GHK equation, a result that is applicable, in general, to other $K^+$ channels as well as other channel types Clay, 2000). The functional significance of the $K^+$ channel GHK result, if any, for neuronal signaling in the central nervous system and perhaps elsewhere, has not been determined. Details of the $K^+$ accumulation/depletion mechanism appear to be specific to squid giant axons, although periaxonal $K^+$ accumulation may play a role in saltatory propagation of action potentials in myelinated axons (Zhou and Chiu, 2001). Axoplasmic accumulation of $Na^+$ may be a significant factor in small axons when the sodium–potassium pump is compromised (Schwarz et al., 1995).

In summary, the original work of Hodgkin and Huxley (1952a–d) continues to exert an influence on the field of membrane excitability and related areas. They applied the voltage-clamp technique in a novel way that revealed the mechanism of cellular excitability. Their idea that the rising phase of the action potential was attributable to voltage-dependent movement of $Na^+$ across nerve membrane, which was based on the observation by Hodgkin and Katz (1949) that the overshoot of the AP went beyond the 0 mV level and was sensitive to $Na_o$, is the centerpiece of our understanding of cellular excitability. Moreover, their description of separate pathways across nerve membrane for $Na^+$ and $K^+$ was without precedent. Furthermore, they implicitly assumed that channel gating and ion permeation through an open channel are independent processes, which has been largely confirmed. Not surprisingly, their detailed descriptions of gating have been superceded by other models, such as that of Vandenberg and Bezanilla (1991a b) for $I_{Na}$ and Zagotta et al. (1994) for $I_K$, which are Markov models containing several states connected by voltage-dependent parameters. The HH $m^3h$ and $n^4$ mechanisms can be described in a similar manner. Consequently, in a global sense, the more recent gating models are not fundamentally different from those of HH.

## Appendix A

The Vandenberg and Bezanilla (1991b) model of $I_{Na}$ is given by

$$I_{Na} = \frac{g'_{Na} p_O V[\exp((V - E_{Na})/24) - 1]}{\{[\exp(V/24) - 1][1 + 0.4\exp(-0.38V/24)]\}} \tag{A.1}$$

with $g'_{Na} = 180\,\mathrm{mS/cm^2}$, $E_{Na} = 55\,\mathrm{mV}$, and $p_O$ is the probability that any given $Na^+$ channel is in the open state (state O) of the Vandenberg and Bezanilla (1991b) model (diagram in the text). The latter quantity can be determined from the following set of equations (which follows directly from the diagram):

$$dp_{C2}/dt = y - (2y + z)p_{C2} + (z - y)p_{C3} - y(p_{C4} + p_{C5} + p_I + p_{I4} + p_{I5}), \tag{A.2}$$

$$dp_{C3}/dt = yp_{C2} - (y + z)p_{C2} + zp_{C4}, \tag{A.3}$$

$$dp_{C4}/dt = yp_{C3} - (a + z + g)p_{C4} + bp_{C5} + jp_{I4}, \tag{A.4}$$

$$dp_{C5}/dt = ap_{C4} - (b + c)p_{C5} + dp_O, \tag{A.5}$$

$$dp_I/dt = -(d + i)p_I + cp_{I5} + fp_O, \tag{A.6}$$

$$dp_{I4}/dt = gp_{C4} - (j + a)p_{I4} + bp_{I5}, \tag{A.7}$$

$$dp_{I5}/dt = dp_I + ap_{I4} - (b + c)p_{I5}, \tag{A.8}$$

$$dp_O/dt = cp_{C5} + ip_I - (d + f)p_O, \tag{A.9}$$

$$p_{C1} = 1 - (p_{C2} + p_{C3} + p_{C4} + p_{C5} + p_I + p_{I4} + p_{I5}) \tag{A.10}$$

with (in $\mathrm{ms^{-1}}$) $a = 7.55\exp(0.017(V - 10))$, $b = 5.6\exp(-0.00017(V - 10))$, $c = 21.0\exp(0.06(v - 10))$, $d = 1.8\exp(-0.02(v - 10))$, $f = 0.56\exp(0.00004(v - 10))$, $j = 0.009\exp(-0.038(V - 10))$, $y = 22.0\exp(0.014(V - 10))$, and $z = 1.26\exp(-0.048(V - 10))$.

## References

Adelman, W.J., Fitzhugh, R., 1975. Solutions of the Hodgkin–Huxley equations modified for potassium ions in a periaxonal space. Fed. Proc. 34, 1322–1329.

Adelman, W.J., Palti, Y., 1969. The influence of external potassium on the inactivation of sodium currents in the giant axon of the squid, *Loligo pealei*. J. Gen. Physiol. 53, 685–703.

Adelman, W.J., Palti, Y., Senft, J.P., 1973. Potassium ion accumulation in a periaxonal space and its effects on the measurement of membrane potassium ion conductance. J. Membr. Biol. 13, 387–410.

Adelman, W.J., Moses, J., Rice, R.V., 1977. An anatomical basis for the resistance and capacitance in series with the excitable membrane of the squid giant axon. J. Neurocytol. 6, 621–646.

Armstrong, C.M., Bezanilla, F., 1973. Currents related to movement of the gating particles of the sodium channels. Nature 242, 459–461.

Armstrong, C.M., Bezanilla, F., 1977. Inactivation of the sodium channel. II. Gating current experiments. J. Gen. Physiol. 70, 567–590.

Attwell, D., Cohen, I., Eisner, D., Ohba, M., Ojeda, C., 1979. The steady-state TTX-sensitive (“window”) sodium current in cardiac Purkinje fibers. Pflugers Arch. 379, 137–142.

Berneche, S., Roux, B., 2001. Energetics of ion conduction through the $K^+$ channel. Nature 414, 73–77.
Bevan, S., Yeats, J., 1991. Protons activate a cation conductance in a sub-population of rat dorsal root ganglion neurons. J. Physiol. 433, 145–161.
Bezanilla, F., Armstrong, C.M., 1977. Inactivation of the sodium channel. I. Sodium current experiments. J. Gen. Physiol. 70, 549–566.
Bezanilla, F., Perozo, E., Papazian, D.M., Stefani, E., 1991. Molecular basis of gating charge immobilization in *Shaker* potassium channels. Science 254, 679–683.
Binstock, L., Goldman, L., 1971. Rectification in instantaneous potassium current–voltage relations in *Myxicola* giant axons. J. Physiol. 217, 517–531.
Blair, E., Erlanger, J., 1932. Responses of axons to brief shocks. Proc. Soc. Exp. Biol. Med. 29, 926–927.
Blaustein, M.P., Lederer, W.J., 1999. Sodium/calcium exchange: its physiological implications. Physiol. Rev. 79, 764–830.
Boron, W., DeWeer, P., 1976. Intracellular pH transients in squid giant axons caused by $CO_2$, $NH_2$, and metabolic inhibitors. J. Gen. Physiol. 67, 91–112.
Brodwick, M.S., Eaton, D.C., 1978. Sodium channel inactivation in squid axons is removed by high internal pH or tyrosine specific reagents. Science 200, 1494–1496.
Cannon, S.C., 2002. Sodium channel gating: no margin for error. Neuron 34, 853–858.
Chiu, S.Y., Ritchie, J.M., Rogart, R.B., Stagg, D., 1979. A quantitative description of membrane currents in rabbit myelinated nerve. J. Physiol. 292, 149–166.
Clancy, C.E., Rudy, Y., 1999. Linking a genetic defect to its cellular phenotype in a cardiac arrhythmia. Nature 400, 566–569.
Clay, J.R., 1977. Monte Carlo simulation of membrane noise: an analysis of fluctuations in graded excitation of nerve membrane. J. Theor. Biol. 64, 671–680.
Clay, J.R., 1988. On the relationship between resting potential and the delayed rectifier in squid axons. Biophys. J. 54, 969–970.
Clay, J.R., 1989. Slow inactivation and reactivation of the $K^+$ channel in squid axons. A tail current analysis. Biophys. J. 55, 407–414.
Clay, J.R., 1990. $I_K$ inactivation is shifted along the voltage axis by changes in the intracellular pH. Biophys. J. 58, 797–801.
Clay, J.R., 1991. A paradox concerning ion permeation of the delayed rectifier potassium ion channel in squid giant axons. J. Physiol. 444, 499–511.
Clay, J.R., 1995. A simple model of $K^+$ channel activation in nerve membrane. J. Theor. Biol. 175, 257–262.
Clay, J.R., 1998. Excitability of the squid giant axon revisited. J. Neurophysiol. 80, 903–913.
Clay, J.R., 2000. Determining $K^+$ channel activation curves from $K^+$ channel currents. Eur. Biophys. J. 29, 555–557.
Clay, J.R., 2003a. On the persistent sodium current in squid giant axons. J. Neurophysiol. 89, 640–644.
Clay, J.R., 2003b. A novel mechanism for irregular firing of a neuron in response to periodic stimulation: irregularity in the absence of noise. J. Comp. Neurosci. 15, 43–51.
Clay, J.R., DeFelice, L.J., 1983. Relationship between membrane excitability and single channel open–close kinetics. Biophys. J. 42, 151–157.
Clay, J.R., Shlesinger, M.F., 1983. Effects of external cesium and rubidium on outward potassium currents in squid axons. Biophys. J. 42, 43–53.
Clay, J.R., Shrier, A., 1999. On the role of subthreshold dynamics in neuronal signaling. J. Theor. Biol. 197, 207–216.
Clay, J.R., Shrier, A., 2001. Action potentials occur spontaneously in squid giant axons with moderately alkaline intracellular pH. Biol. Bull. 201, 186–192.
Clay, J.R., Shrier, A., 2002. Temperature dependence of bistability in squid giant axons with alkaline intracellular pH. J. Membr. Biol. 187, 213–233.
Cole, K.S., Moore, J.W., 1960. Potassium ion current in the squid giant axon: dynamic characteristic. Biophys. J. 1, 1–14.
Cole, K.S., Antosiewicz, H.A., Rabinowitz, P., 1955. Automatic computation of nerve excitation. J. Soc. Ind. Appl. Math. 3, 135–172.

Cole, K.S., Guttman, R., Bezanilla, F., 1970. Nerve membrane excitation without threshold. Proc. Natl. Acad. Sci. USA 65, 884–891.

Connor, J.A., 1975. Neural repetitive firing: a comparative study of membrane properties of crustacean walking leg axons. J. Neurophysiol. 38, 922–932.

Connor, J.A., Stevens, C.F., 1971. Prediction of repetitive firing behavior from voltage clamp data on an isolated neuron soma. J. Physiol. 213, 31–53.

Conti, F., Neher, E., 1980. Single channel recordings of $K^+$ current in squid axons. Nature 285, 140–143.

Conti, F., DeFelice, L.J., Wanke, E., 1975. Potassium and sodium ion current noise in the membrane of the squid giant axon. J. Physiol. 248, 45–82.

Conti, F., Hille, B., Neumke, B., Nonner, W., Stampfli, R., 1976. Measurement of the conductance of the sodium channel from current fluctuations at the node of Ranvier. J. Physiol. 262, 699–727.

Crill, W.E., 1996. Persistent sodium current in mammalian central neurons. Annu. Rev. Physiol. 58, 349–362.

DeWeer, P., Geduldig, D., 1978. Contribution of sodium pump to resting potential of squid giant axon. Am. J. Physiol. 235, C55–62.

DiPolo, R., Beauge, L., 2002. Intracellular ionic and metabolic regulation of squid nerve $Na^+/Ca^{+2}$ exchanger. Ann. NY Acad. Sci. 976, 224–236.

Doyle, D.A., Morais-Cabral, J., Pfuetzner, R.A., Kuo, A., Gulbis, J.M., Cohen, S.L., Chait, B.T., MacKinnon, R., 1998. The structure of the potassium channel: molecular basis of $K^+$ conductance and selectivity. Science 280, 69–77.

Ehrenstein, G., Gilbert, D.L., 1966. Slow changes of potassium permeability in the squid giant axon. Biophys. J. 6, 553–566.

Fitzhugh, R., 1955. Mathematical models of threshold phenomena in the nerve membrane. Bull. Math. Biophys. 17, 257–278.

Fitzhugh, R., 1961. Impulses and physiological states in theoretical models of nerve membrane. Biophys. J. 1, 445–466.

Fitzhugh, R., Antosiewicz, H.A., 1959. Automatic computation of nerve excitation-detailed corrections and additions. J. Soc. Ind. Appl. Math. 7, 447–458.

Frankenhauser, B., 1962. Potassium permeability in myelinated nerve fibers of *Xenopus laevis*. J. Physiol. 160, 54–61.

Frankenhauser, B., Hodgkin, A.L., 1956. The after-effects of impulses in the giant nerve fibers of *Loligo*. J. Physiol. 131, 341–376.

Frankenhauser, B., Huxley, A.F., 1964. The action potential in the myelinated nerve fiber of *Xenopus laevis* as computed on the basis of voltage-clamp data. J. Physiol. 171, 302–315.

Gerstein, G.L., Mandelbrot, B., 1964. Random walk models for the spike activity of a single neuron. Biophys. J. 4, 41–68.

Goldman, D.E., 1943. Potential, impedance, and rectification in membranes. J. Gen. Physiol. 27, 37–60.

Guckenheimer, J., Oliva, R.A., 2002. Chaos in the Hodgkin–Huxley model. SIAM J. Appl. Dyn. Systems 1, 105–114.

Guttman, R.S., Barnhill, R., 1970. Oscillation and repetitive firing in squid axons. J. Gen. Physiol. 55, 104–118.

Hindmarsh, J.L., Rose, R.M., 1982. A model of the nerve impulse using two first order differential equations. Nature 296, 162–164.

Hodgkin, A.L., 1948. The local electrical changes associated with repetitive action in a non-medullated axon. J. Physiol. 107, 165–181.

Hodgkin, A.L., Huxley, A.F., 1952a. Currents carried by sodium and potassium ions through the membrane of the giant axon of *Loligo*. J. Physiol. 116, 449–472.

Hodgkin, A.L., Huxley, A.F., 1952b. The components of membrane conductance in the giant axon of *Loligo*. J. Physiol. 116, 473–496.

Hodgkin, A.L., Huxley, A.F., 1952c. The dual effect of membrane potential on sodium conductance in the giant axon of *Loligo*. J. Physiol. 116, 497–506.

Hodgkin, A.L., Huxley, A.F., 1952d. A quantitative description of membrane current and its application to conduction and excitation in nerve. J. Physiol. 117, 500–544.

Hodgkin, A.L., Katz, B., 1949. The effect of sodium ions on the electrical activity of the giant axon of the squid. J. Physiol. 108, 37–77.

Hodgkin, A.L., Keynes, R.D., 1955. The potassium permeability of a giant nerve fiber. J. Physiol. 128, 61–88.

Horn, R., 1999. The dual role of calcium—pore blocker and modulator of gating. Proc. Natl. Acad. Sci. USA 96, 3331–3332.
Hoyt, R., 1982. Origin of the rising phase of gating currents. Biophys. J. 40, 251–254.
Huxley, A.F., 1959. Ion movements during nerve activity. Ann. NY Acad. Sci. 81, 221–246.
Inoue, I., 1985. Voltage-dependent chloride conductance of the squid axon membrane and its blockade by some disulfonic stilbene derivatives. J. Gen. Physiol. 85, 519–537.
Kaplan, D., Clay, J.R., Manning, T., Glass, L., Guevara, M.R., Shrier, A., 1996. Subthreshold dynamics in periodically stimulated squid giant axons. Phys. Rev. Lett. 76, 4074–4077.
Kimura, J.E., Meves, H., 1979. The effect of temperature on the asymmetrical charge movement in squid giant axons. J. Physiol. 289, 479–500.
Lecar, H., Nossal, R., 1971a. Theory of threshold fluctuations in nerves. I. Relationship between electrical noise and fluctuations in axon firing. Biophys. J. 11, 1048–1067.
Lecar, H., Nossal, R., 1971b. Theory of threshold fluctuations in nerve. II. Analysis of various sources of membrane noise. Biophys. J. 11, 1068–1084.
Lossin, C., Wang, D.W., Rhodes, T.H., Vanoye, C.G., George Jr., A.L., 2002. Molecular basis of an inherited epilepsy. Neuron 34, 877–884.
Monnier, A., Jasper, H., 1932. Recherche de la rélation entre les potentials d'action élémentaires et la chronaxie de subordination. Nouvelle demonstration du fonctionnement par 'tout ou rien' de la fibre nerveuse. C. R. Soc. Biol. Paris 110, 547–549.
Mozhayeva, G.N., Naumov, A.P., Khodorov, B.I., 1982. Potential dependent blockade of batrachotoxin-modified sodium channels in frog node of Ranvier by calcium ions. Gen. Physiol. Biophys. 1, 281–282.
Nagumo, J.S., Arimoto, S., Yoshizawa, S., 1962. An active pulse transmission line simulating nerve axon. Proc. IRE 50, 2061–2070.
Nonner, W., Rojas, E., Stampfli, R., 1975. Displacement currents in the node of Ranvier. Voltage and time dependence. Pflugers Arch. 354, 1–18.
Otis, T.S., Gilly, W.F., 1990. Jet-propelled escape in the squid *Loligo opalescens*: concerted control by giant and non-giant motor axon pathways. Proc. Natl. Acad. Sci. USA 87, 2911–2915.
Oxford, G.S., 1981. Some kinetic and steady-state properties of sodium channels after removal of inactivation. J. Gen. Physiol. 77, 1–22.
Patlak, J.B., 1991. Molecular kinetics of the voltage-dependent $Na^+$ channel. Physiol. Rev. 71, 1047–1080.
Poussart, D., 1971. Membrane current noise in lobster axon under voltage clamp. Biophys. J. 11, 211–234.
Rakowski, R.F., Gadsby, D.C., DeWeer, P., 1989. Stoichiometry and voltage-dependence of the sodium pump in voltage-clamped, internally dialyzed squid giant axon. J. Gen. Physiol. 93, 903–941.
Rakowski, R.F., Gadsby, D.C., DeWeer, P., 2002. Single ion occupancy and steady-state gating of Na channels in squid giant axons. J. Gen. Physiol. 119, 235–249.
Reyes, A.D., Fetz, E.E., 1993a. Two modes of interspike interval shortening by brief transient depolarizations in cat neocortical neurons. J. Neurophysiol. 69, 1661–1672.
Reyes, A.D., Fetz, E.E., 1993b. Effects of transient depolarizing potentials on the firing rate of cat neocortical neurons. J. Neurophysiol. 69, 1673–1683.
Rinzel, J., 1978. On repetitive firing in nerve. Fed. Proc. 3, 2793–2802.
Rudy, B., 1978. Slow inactivation of the sodium conductance in squid giant axon: pronase resistance. J. Physiol. 283, 1–21.
Rudy, B., 1988. Diversity and ubiquity of K channels. Neuroscience 25, 729–749.
Schneidman, E., Freedman, B., Segev, I., 1998. Ion-channel stochasticity may be critical in determining the reliability and precision of spike timing. Neural Comput. 10, 1679–1703.
Schumaker, M.F., MacKinnon, R., 1990. A simple model for multi-ion permeation. Single-vacancy conduction in a simple pore model. Biophys. J. 58, 975–984.
Schwarz, J.R., Reid, G., Bostok, H., 1995. Action potentials and membrane currents in the human node of Ranvier. Pflugers Arch. 430, 283–292.
Sigworth, F.J., 1980. The variance of sodium current fluctuations at the node of Ranvier. J. Physiol. 307, 97–129.
Sigworth, F.J., 2003. Structural biology: life's transistors. Nature 423, 21.

Sigworth, F.J., Neher, E., 1980. Single $Na^+$ channel currents observed in cultured rat muscle-cells. Nature 287, 447–449.

Steinmetz, P.N., Manwani, A., Koch, C., London, M., Segev, I., 2000. Subthreshold voltage noise due to channel fluctuations in active neuronal membranes. J. Comp. Neurosci. 9, 133–148.

Strassberg, A.F., DeFelice, L.J., 1993. Limitations of the Hodgkin–Huxley formalism: effect of single channel kinetics on transmembrane voltage dynamics. Neural Comput. 5, 843–855.

Taglialatela, M., Stefani, E., 1993. Gating currents of the cloned delayed rectifier $K^+$ channel. Proc. Natl. Acad. Sci. USA 90, 4758–4762.

Tuckwell, H.C., 1988. Introduction to Theoretical Neurobiology. Cambridge University Press, Cambridge.

Vandenberg, C.A., Bezanilla, F., 1991a. Single-channel, macroscopic, and gating currents from sodium channels in the squid giant axon. Biophys. J. 60, 1499–1510.

Vandenberg, C.A., Bezanilla, F., 1991b. A sodium channel gating model based on single-channel, macroscopic, ionic, and gating currents in the squid giant axon. Biophys. J. 60, 1511–1533.

Wanke, E., Carbone, E., Testa, P.L., 1980a. The sodium channel and intracellular $H^+$ blockage in squid axons. Nature 287, 62–63.

Wanke, E., Carbone, E., Testa, P.L., 1980b. $K^+$ conductance modified by a titratable group accessible to protons from the intracellular side of the squid axon membrane. Biophys. J. 26, 319–324.

Wolfram, S., 1999. The Mathematica Book 4th Edition. Wolfram Media/Cambridge University Press, New York.

Yamamoto, D.K., Yeh, J.Z., Narahashi, T., 1984. Voltage-dependent calcium block of normal and tetramethrin-modified single sodium channels. Biophys. J. 45, 337–344.

Zagotta, W.N., Hoshi, T., Aldrich, R.W., 1994. Shaker potassium channel gating. III: evaluation of kinetic models for activation. J. Gen. Physiol. 103, 279–319.

Zhou, L., Chiu, S.Y., 2001. Computer model for action potential propagation through branch point in myelinated nerves. J. Neurophysiol. 85, 197–210.

Zhou, Y., Morais-Cabral, J.H., Kaufman, A., MacKinnon, R., 2001. Chemistry of ion coordination and hydration revealed by a $K^+$ channel-Fab complex at 2.0 Å resolution. Nature 414, 43–48.